Schedule Reliability in Liner Shipping Timetable Design: A Convex Programming Approach

Abraham Zhang,[*] Zhichao Zheng,[†] Chung-Piaw Teo[‡]

Abstract

Container liner shipping is the primary mode of moving manufactured products across continents. Partly due to inherent uncertainties at sea and ports, the liner shipping industry has long had a notorious reputation of schedule delays and unreliable on-time performance. This paper formulates a new approach to incorporate schedule reliability targets in liner shipping timetable design, to balance bunker consumption, time taken for the voyage, and schedule delays. We first model a surrogate problem using a copositive program through a moment decomposition approach and solve it as a convex semidefinite programming relaxation. We next incorporate schedule reliability targets implicitly by exploiting the optimality condition of this surrogate model.

We use this approach to analyze the trade-offs between the bunker consumption and the schedule reliability targets for each port call. Furthermore, we derive the optimal speed of the vessel in each leg of the schedule to control for total bunker consumption. Surprisingly, the analytical analysis shows that, if a shipping line has the freedom to choose its preferred berthing times at all ports, it is optimal to set design sailing speeds equal at all legs to maximize schedule reliability.

We validate our model using data from a Daily Maersk service, and demonstrate that our schedule can achieve an even higher schedule reliability than the innovative Daily Maersk service schedule, which attained more than 98% reliability in practice, with 11.4% lower bunker consumption. In comparison with a common schedule design heuristic, our model can design service schedules that improve the reliability performance by at least five percentage points, consuming the same amount of bunker. For the same reliability target (of 80%) in schedule design, our model can help reduce bunker consumption by about 11.6% for an 11-week schedule. The savings in bunker consumption can be much more substantial when an ocean carrier aims for higher schedule reliability.

Key words: Schedule reliability; bunker consumption; liner shipping; distributionally robust optimization; copositive program

[*]Essex Business School, University of Essex, Elmer Approach, Southend-on-Sea, Essex, SS1 1LW, United Kingdom
[†]Lee Kong Chian School of Business, Singapore Management University, 50 Stamford Road, Singapore 178899, Singapore
[‡]Institute of Operations Research and Analytics, National University of Singapore, 15 Kent Ridge Drive, Singapore 119245, Singapore

1 Introduction

Since its intervention in the 1950s, container liner shipping has grown to be the primary mode of moving manufactured products across continents (Notteboom & Rodrigue, 2008). As more operations are outsourced and an increasing share of goods is containerized, container liner shipping is now the lifeline of most, if not all, global supply chains (Fransoo & Lee, 2013). The service quality of container liner shipping services, thus, plays a key part in influencing global supply chain performance.

A standard liner shipping service has a weekly sailing frequency and calls at several ports. Although it is a routine for shipping lines to publish in advance their service port calls and schedules, the liner shipping industry has long had a notorious reputation of schedule unreliability. In the 2019 Schedule Reliability Report published by eeSea, the global liner schedule on-time performance averaged at 47% with the best performance at only 65%, where the on-time performance counts both arriving early and less than 8 hours delay[1]. This corresponded to 1.6 days delay on average across 2019. Such low schedule reliability forces shippers to keep substantial safety stocks (Vernimmen et al., 2007; Zhang & Lam, 2014, 2015), and makes it nearly impossible for shippers to practice efficient just-in-time production/distribution as long as maritime container transport is involved (Lam & van de Voorde, 2011).

Schedule unreliability in liner shipping has its root in the inherent operational challenges. A container vessel faces many uncertainties at sea, for example, extreme weather conditions, adverse sea conditions including currents and tides, etc. A vessel's schedule integrity is also affected by uncertainties at ports. A vessel's port time is stochastic because the number of containers to be loaded/unloaded is not known exactly at the planning stage, and port handling productivity fluctuates. More importantly, container port congestion is commonplace and berth waiting time may be prolonged and hard to predict (Notteboom, 2006). This problem is further exaggerated as delays are often propagated in the subsequent port calls. For these reasons, many industry professionals are skeptical if it is ever possible to ensure schedule integrity in maritime container transport.

This study is motivated by the experience of the Daily Maersk service, which was rolled out in late 2011. Promising "absolute reliability" (100% reliability), Maersk Line, the world's largest shipping line, increased its share of the very competitive Asia-Europe trade from 21% to 25% six months after the launch of the new service (Leach, 2012). This clearly shows that schedule reliability is a market winning factor. In fact, there is a growing trend for shippers to value schedule reliability more than a low freight rate. For this reason, Eivind Kolding, the former chief executive of Maersk Line, stated in 2011 that "Reliability is the new rate war; we need an end-to-end view on reliability". This implies that shipping lines must understand the strategic importance of schedule reliability. They also need to improve their operations continuously to survive fierce competition. Unfortunately, Maersk had to drop the Daily Maersk service in 2015 as "Maersk had found that customers were not willing to pay a higher price

---

[1] https://www.eesea.com/schedule-reliability-report

2

for better service... We had a lot of extra costs to deliver that level of reliability, so we have changed our strategy."[2] Therefore, it is utmost important in practice to balance the trade-off between schedule reliability and operating costs.

In academia, research studies of liner ship scheduling have given the most attention to cost, as can be observed in the reviews of Christiansen et al. (2004) and Kjeldsen (2011). The phenomenon may be explained by the traditional cost focus of shipping lines, as ocean container transport has long been viewed as a commoditized service. The upward trend in fuel price in the first decade of the new millennium sparked research studies that minimize fuel consumption (Qi & Song, 2012) or total operating cost (Wang & Meng, 2012a,b). However, little research has been devoted to schedule reliability, which has become increasingly important for efficient global supply chains. Big data firms such as ClipperData and eeSea have been tracking ships with AIS and terminal data, etc., reporting the performance of different service schedules (see Figure 1), and influencing the shippers in their choice of carriers in the process.

Figure 1: Big data platform from ClipperData capturing duration, schedule reliability, fuel efficiency and other features of each route in the shipping lines.

We study the problem of scheduling container liner ships to meet voyage duration, bunker consumption, and schedule reliability targets at selected ports. Port calls and port rotation are given. The journey time T of a round-trip voyage is predetermined; for example, it is often 11 weeks for a Fast East-Europe service. The bunker consumption budget of B is also predetermined. The reliability target at each port call is also fixed—we want the on-time arrival probability to be at least η_i for port i. Note that η_{I+1} denotes the probability target that the vessel will return back to the first port on time at the end of time T. The key question we address in this paper is:

Problem (Q): *Suppose a vessel with given port calls leaves the first port promptly at the beginning of the time horizon (i.e., $\eta_1 = 1$). Design a timetable for the voyage to determine*

3

the schedule and sailing speed of each leg (if feasible) so that the total voyage time is T, the schedule reliability (on-time arrival probability) at each port is at least (η_i), and total bunker consumption is at most B.

Note that this is a feasibility problem with no objective to optimize. Our focus here is the trade-off between bunker consumption and schedule reliability. The research question aims to determine whether a set of reliability targets is feasible or not given a limited bunker budget. Although liner schedule design is not a new problem, to the best of our knowledge, Problem (Q) is still unsolved in the literature, and there is little understanding of the structural properties of the optimal schedules in the stochastic environment. It is even unknown if the bunker consumption budget B, voyage time constraint T, and reliability targets $\{\eta_i : i = 1, \ldots, I + 1\}$ are viable. The closest we know is the work of Qi (2017), who studies a version of schedule reliability in the healthcare appointment scheduling problem. However, due to the difficulty of modeling the impact of delay propagation in this class of problem, the author can only analyze the problem under a max-min objective, instead of the more refined differentiated reliability targets posed in this paper.

We choose bunker consumption as a target measure instead of a bunker cost because of two reasons. First, bunker consumption is directly linked to the environmental impact of the shipping line operations, which has received increasing attention from both the industries and the general public (Du et al., 2015). Second, the bunker cost is subject to various risks from the global financial and political environments. Shipping lines usually adopt specific hedging approaches to mitigate these risks, which is generally beyond the scope of the schedule decisions. In this paper, we would like to focus on the schedule design problem given a route and understand the trade-off between bunker consumption and schedule reliability by solely considering operational risks. Nevertheless, we show in Section 4.1 that our model can be extended to capture the budget in bunker cost with uncertain bunker price.

Schedule reliability is measure by the difference between the schedule and the (random) arrival times, which are often caused by port time and sailing time variation against the norm. Figure 2 is a box-plot of the port times in several ports in the world. The port times are quite random and of varying patterns. This extends to the travel time between ports. Furthermore, most catastrophic disruptions to the schedule are caused by extreme weather conditions, like typhoons, which are rare and difficult to forecast at the schedule planning stage. Therefore, we employ a distributionally robust optimization (DRO) approach to design a schedule that achieves the best performance under the worst possible distribution of the uncertainty. Instead of using an estimated distribution for the uncertainty, which could subject to significant estimation errors due to insufficient data, the DRO framework assumes that the uncertain parameters could follow any distribution that satisfies some common distributional conditions, like sharing the same mean and variance, etc. The DRO solution aims to optimize the objective function under the worst possible distribution. Note that the worst-case distribution could be different for

different feasible solutions. This provides a lower bound or a worst-case performance guarantee for the liner schedules, even under extreme scenarios, which aligns with the objective of absolute reliability. We apply a reformulation technique that transforms the problem into a convex optimization problem, which allows us to characterize the structure of the optimal solution from the optimality conditions of convex programming problems.
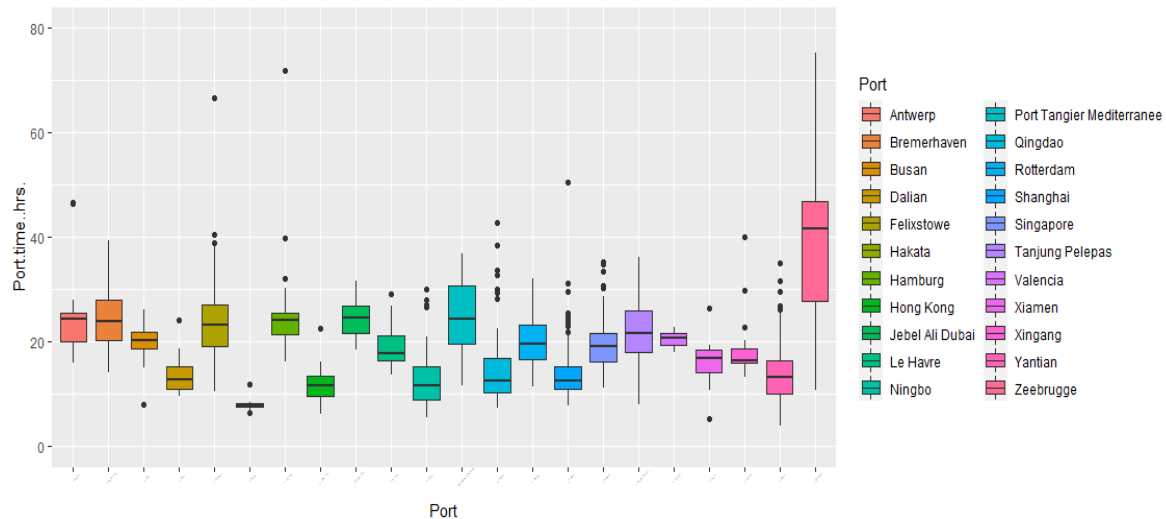

Figure 2: Port times at different ports in the world based on data from the Maersk Line

The contributions of this paper are multi-fold. First, to the best of our knowledge, this paper is the first attempt to model the liner scheduling problem using a DRO framework. Second, we design an innovative solution approach based on the optimality conditions of the convex reformulation of DRO formulation. Specifically, we first develop a surrogate model to minimize the expected weighted sum of the delay time at each port using the DRO framework. Next, by analyzing the optimality conditions of the DRO model, we recover the on-time probability as a function of the weights on the delay times, based on which we design an iterative search algorithm to obtain a schedule that delivers the on-time probability targets (if feasible), i.e., solving Problem (Q). Third, we show that the optimal sailing speed for each leg is identical in a liner service route and that when there is a voyage time limit on the headhaul route, there will be two optimal sailing speeds for headhaul legs and backhaul legs. This differs our paper from the general appointment scheduling literature and contributes to the understanding of liner service planning in practice, where typically a nominal speed (sometimes one for headhaul and another for backhaul) is used at the planning stage.

The rest of this paper is organized as follows. Section 2 reviews relevant literature. Section 3 describes our schedule reliability model, followed by the analysis of reliability targets and optimal sailing speeds. Extensions of the model to capture uncertain bunker prices, shipping network planning and nonidentical bunker consumption functions are discussed in Section 4. Section 5 validates our approach via simulation experiments using real data from practice. Insights from our model and numerical results are discussed

5

in Section 6. Section 7 concludes the research and suggests areas for further investigation.

2   Literature Review

Research in liner shipping schedule design has focused on cost minimization or profit maximization. According to the reviews of Christiansen et al. (2004) and Kjeldsen (2011), all the relevant early publications either minimized cost or maximized profit. Some of the works did not consider uncertainties. For example, Agarwal & Ergun (2008) formulated a mixed-integer linear program to solve the ship-scheduling and the cargo-routing problems simultaneously to maximize operating profit. Agarwal & Ergun (2010) studied the problem of network design and mechanisms for capacity allocation in liner shipping alliances. Fagerholt et al. (2010) used the shortest path approach to solve a nonlinear continuous program for reducing fuel emissions by optimizing speed on shipping routes. Wang & Meng (2012c) optimized sailing speed for container ships on each leg of each ship route in a liner shipping network to minimize total operating cost.

Driven by the increased bunker prices and pressure on emissions reduction, some studies investigated the impact of uncertainties in bunker prices to reduce bunker costs or emissions. Among them, Notteboom & Vernimmen (2009) and Ronen (2011) analyzed the effect of rising bunker prices on liner service configuration. They suggested reducing sailing speed and adding more vessels in service design. Yao et al. (2012) studied bunker fuel management strategies, including ship speeds adjustment, for minimizing bunker consumption. Wang et al. (2013) reviewed and extended several methods for optimizing bunker consumption in shipping. Du et al. (2015) dealt with bunker budget and minimized fuel consumption over a round voyage via robust optimization. Wang et al. (2018) jointly optimized sailing speed and bunker purchase with distribution-free stochastic bunker prices. Given the difficulties in calibrating bunker prices into a specific joint probability distribution, they used approximation techniques based on the descriptive statistics of historical bunker prices.

More recent works integrated uncertain time factors in their models. For instance, Wang & Meng (2012a) formulated a mixed-integer nonlinear stochastic programming model to hedge against uncertainties in port operations to minimize the ship costs, the expected bunker costs, plus late start handling costs. Through sensitivity analysis, it analyzed the impact of the number of ships deployed on the schedule robustness. Wang & Meng (2012b) developed a mixed-integer nonlinear stochastic programming model with sea contingency time and port time uncertainty. The model minimized the vessel cost and expected bunker cost while maintaining a required transit time service level. Qi & Song (2012) employed simulation-based stochastic approximation methods to minimize fuel emissions by optimizing vessel schedules with uncertain port times. Lee et al. (2015) analyzed the impact of slow ocean steaming on delivery reliability and fuel consumption. They concluded that slow steaming with the flexibility to

6

speed up helps improve delivery reliability amid uncertainties in port and sailing times. Note that slow steaming refers to the practice of reducing sailing speed from a typical 24 knots to 21 knots or under (Maloni et al., 2013). Song et al. (2015) developed a stochastic multi-objective model to decide on the number of ships, the planned maximum sailing speed, and the liner service schedule. The objectives were to simultaneously optimize the expected cost, the schedule reliability and the shipping emission in the presence of port time uncertainty, and the authors solved the model using a genetic algorithm.

More recently, Aydin et al. (2017) used dynamic programming to optimize sailing speeds and bunkering decisions considering uncertain service times and time windows at ports. Their model minimizes the total fuel consumption while maintaining schedule reliability. Mulder et al. (2019) developed a stochastic dynamic program to optimize speed and buffer times in schedule design simultaneously. The cost optimization objective included the costs of delayed port arrivals and departures and the sailing costs of (optimally) performing recovery actions such as speed adjustments. The authors assumed discrete model primitives and used long-run average analysis to tackle the problem. Mulder & Dekker (2019) extended the model in Mulder et al. (2019) to capture port skipping options and both convex and concave cost functions. The authors further extended the model formulation to include chance constraints on delay probabilities. However, their models are based on the Markov decision process (MDP) that assumes Markov transition of the system states, which does not capture any correlation among the uncertainties in different legs. Furthermore, the model formulation relies on the steady-state probabilities, which are unlikely to exist given the long period of finishing a shipping route.

Applications of the above paper either require making assumptions on uncertain time factors' probability distributions or using sample-average approximation. In reality, port times and sailing delays may not fit any probability distribution, and the data could be insufficient to represent unseen future scenarios. Our work overcomes this issue by using a DRO methodology. Furthermore, inspired by Daily Maersk's "absolute reliability" ambition, we aim to find a schedule (if feasible) to achieve given target schedule reliability (on-time arrival probability), which differs from most works. We explicitly capture the trade-off in bunker consumption and schedule reliability by imposing an upper limit on bunker consumption in the model. Our modeling approach enables us to generate fresh insights on liner shipping schedule design.

Under the DRO framework, the uncertain parameters follow a joint distribution that is drawn from a set of distributions, called the ambiguity set, and decision-maker aims to find the optimal decision whose performance is guaranteed under the worst-case distribution. There are various ways of characterizing the ambiguity set of distributions. For example, the set of distributions can contain any distribution whose distance from a nominal distribution is bounded by a given number under certain measures. The Wasserstein DRO models, which is increasingly popular in the machine learning field, fall under this category with the distance between distributions measured by the Wasserstein distance (Gao & Kley-

wegt, 2016; Hanasusanto & Kuhn, 2017; Mohajerin Esfahani et al., 2018; Chen et al., 2018; Kuhn et al., 2019). Another stream of DRO models describes the ambiguity set of distributions using common distributional information—e.g., the ambiguity set may contain distributions that share the same moments and support or follow the same marginal distributions (Delage & Ye, 2010; Li et al., 2014). These DRO models have been applied in various contexts, including project management (Natarajan et al., 2011), healthcare appointment scheduling (Kong et al., 2013), consumer choice models (Mishra et al., 2011), traffic equilibrium analysis (Ahipaşaoğlu et al., 2016), workforce deployment (Yan et al., 2017), and supply chain risk management (Gao et al., 2019), etc.

In this paper, we adopt the moment-based approach to describe the uncertain parameters arising in the liner scheduling problems as the moment information (e.g., mean and standard deviation) is easier to interpret in the shipping context and can be estimated rather reliably from the historical data on schedule performance. In particular, we model the port time uncertain and extreme weather disruption using the moment-based DRO framework and follow the conic programming reformulation techniques to transform the DRO version of the liner scheduling problem into a deterministic convex optimization model. We further extend the model to capture the uncertainty in bunker prices at different ports. This paper contributes to the DRO literature by formulating the distributionally robust liner schedule reliability problem and demonstrating how to calibrate key model inputs through an innovative search algorithm based on the optimality conditions from the conic reformulation of the DRO model. In the traditional DRO model, the probabilistic constraints in the reliability targets are also incorporated through explicit additional constraints via various methods for convex approximation. Here we capture these constraints directly in a new way through the optimality conditions in our DRO model.

The liner scheduling problem is similar to the appointment scheduling problem in healthcare settings, including outpatient services and operating theaters (Cayirli & Veral, 2003; Gupta & Denton, 2008). In the healthcare appointment scheduling problems, the decision is usually to assign appointment times for a set of patients to arrive at the service locations, and the uncertainties could arise from random service duration, patient no-show behavior, and unpunctual arrivals, etc. The decision-maker typically designs the appointment systems to balance the trade-off between patient waiting time, system idling time and overtime. There is also a stream of literature that tries to apply the DRO approach to solve the healthcare appointment scheduling problems (Kong et al., 2013; Mak et al., 2015; Bertsimas et al., 2019). Despite the similarities between these two scheduling problems, a key feature in our problem that differs from healthcare appointment scheduling problems is that we also need to design the vessel's sailing speed in each leg, and the sailing speeds affect the bunker consumption in a nonlinear way. The analog decision of sailing speed in the healthcare setting would be the service (e.g., consultation or surgery) speed of the physicians for each patient, which usually is given exogenously and cannot be optimized by the decision-maker. The main trade-off in our liner scheduling problem is between schedule reliability

8

and energy efficiency measured by bunker consumption, which is also very different from the trade-off concerned in the healthcare appointment scheduling problems.

3 Schedule Reliability Model

The liner shipping industry currently measures schedule reliability by on-time probability or mean arrival delay time. A ship is considered on time if it arrives at the port of destination on the scheduled day or the day immediately before the scheduled day of arrival (Notteboom & Rodrigue, 2008). The measurement of on-time probability does not take into account the differences in delay times. For example, a delay of 1 day and a delay of 1 week have the same impact on on-time probability. However, they may have very different implications for shippers, terminal operators and ocean carriers. Analyzing the on-time probability is already a difficult computational problem even with a fixed schedule. For this reason, we first solve a surrogate model that measures schedule reliability by mean arrival delay instead of on-time probability. Specifically, the surrogate model minimizes the expected weighted sum of delay time at each port. Note that our original research problem is a feasibility problem, but the surrogate model has a specific objective to optimize. We show later in our model analysis that we can link the on-time probabilities to the weights on delay times in the objective function, which in turn allows us to calibrate the weights so that the surrogate model can produce a schedule that achieves the on-time probability targets (if feasible). In this way, we solve the original feasibility problem, i.e., Problem (Q).

3.1 Surrogate Problem Formulation

Let I denote the total number of port calls in the route. The home port is defined as the 1st port of call. The ith leg is defined as the voyage from the ith port of call to the $(i+1)^{\text{th}}$ port of call, where $i = 1, 2, \ldots, I - 1$, and the Ith leg is from the Ith port of call back to the home port. For the convenience of notation, sometimes we also refer to the home port as the $(I+1)^{\text{th}}$ port of call when it means the last port at the end of the voyage. The planned round-trip journey time, T, is determined by the fleet size, i.e., the number of weeks for the round-trip time equals the number of vessels required. During the timetable design stage, we assume that a ship maintains a fixed sailing speed in each leg of the voyage, which is a common practice in the schedule planning of container ships (Du et al., 2011). Our model chooses the optimal sailing speed for each leg, subject to the total bunker consumption constraint.

Note that in actual operations, shipping lines often vary the sailing speed dynamically to minimize cost and to catch up on the schedule. We do not consider these recovery decisions at the *operational level* as our model focuses on timetable design which is mainly a *tactical level* decision. Note that our moment decomposition approach based on real data has already captured the impact of these recovery operations implicitly - the port times and sailing times in adjacent legs are highly correlated because a

delay in one port will likely lead to shortened port and sailing time in the next port, due to the recovery operations employed by shipping lines.

Bunker Consumption

Let v_i represent the designed sailing speed on the ith leg, and it is limited between v_i^{min} and v_i^{max}. It is well known that bunker consumption rate is typically a cubic function of sailing speed (Ronen, 1982; Fagerholt et al., 2010). In our schedule design problem, we consider a bunker consumption budget for the route, denoted as B. Then the constraint on bunker consumption can be represented as follows:

$$\sum_{i=1}^{I} \frac{D_i}{v_i} \left(k_1 v_i^3 + k_2 v_i^2 + k_3 v_i + k_4 \right) \leq B, \text{ i.e., } \sum_{i=1}^{I} D_i \left(k_1 v_i^2 + k_2 v_i + k_3 + \frac{k_4}{v_i} \right) \leq B, \tag{1}$$

where k_1, k_2, k_3 and k_4 are some constants; and D_i is the sailing distance of the ith leg. For all the consumption functions estimated in the literature, $k_1 > 0$ and $k_4 \geq 0$ (Ronen, 1982; Fagerholt et al., 2010; Du et al., 2011, etc.). The first inequality implies that the bunker consumption eventually will increase as the sailing speed increases, and the second inequality ensures that the bunker consumption will not be negative when the vessel stays still at sea[3]. The actual bunker consumption of a voyage may not strictly obey the given formula because weather conditions, ship payload and other factors can affect bunker consumption, but the given formula is widely regarded as a good approximation. It is also necessary to use a model to quantify the relation between sailing speed and bunker consumption to control the bunker consumption at the timetable design stage. In the practice of slow steaming, the bunker consumption can be saved by slowing down the vessels from their maximum sailing speeds, which implies that even for certain (very rare) types of vessels whose bunker consumption can be reduced by speeding up to a certain threshold, their bunker consumption will eventually increase if the sailing speed exceeds such threshold (Du et al., 2011). Therefore, it is always the case that the maximum speed of a vessel is larger than such threshold (if exists). Note that constraint (1) is highly nonlinear and even not necessarily convex, since we do not impose additional assumptions on the values of the coefficients. We show in our model reformulation that this constraint can be convexified and expressed as a set of convex conic constraints using properties of the optimal solution.

Schedule Reliability

Let $\tilde{\tau}_i$ denote the stochastic service time at the the ith port, and $\tilde{\xi}_i$ be the actual sailing time on the ith leg defined as $\tilde{\xi}_i = D_i/v_i + \tilde{\epsilon}_i$, where $\tilde{\epsilon}_i$ is the random noise in the sailing time mainly due to external conditions. In our study, we focus on adverse weather conditions because they are the primary source of sailing time uncertainty. They are beyond the control of human beings and may have a significant impact on operational performance compared to other sources of noise, like the current. Since the impact

---

[3]When the vessel stays still, the engine may be still working to provide energy for various equipment and systems on the vessel.

10

of adverse weather conditions usually comes in the form of waiting or reduced sailing speed in the sea, it is valid to assume an additive form of uncertainty in the sailing time.

Denote the scheduled arrival time at the ith port by a_i. Then the scheduled arrival time interval between the ith and $(i+1)^{\text{th}}$ port is $x_i = a_{i+1} - a_i$. Thus, we can make a change in variables and let x_i's be the decision variables in our problem. Then we have the voyage time constraint, $\sum_{i=1}^{I} x_i = T$, i.e., $a_{I+1} = T$. Let $\tilde{\alpha}_i$ be the actual arrival time at the ith port. Following the literature, we assume that a port will not service a ship until its scheduled arrival time (Wang & Meng, 2012a). If a ship arrives early, the waiting time is not included in the port service time. This is because terminal handling capacity is a bottleneck in liner shipping and ports/terminals schedule time windows for ships. A ship that arrives early at a port usually has to wait until its assigned time window for berthing (Qi & Song, 2012). This means that buffer time not utilized in the previous leg will be forfeited and can not be carried over to the next leg. Therefore, $\tilde{\alpha}_i$ is given by the following recursive formula:

$$\tilde{\alpha}_{i+1} = \max\{\tilde{\alpha}_i, a_i\} + \tilde{\tau}_i + \tilde{\xi}_i, \forall i = 1, 2, \ldots, I-1,$$

where $\max\{\tilde{\alpha}_i, a_i\}$ indicates the starting time of unloading/loading at the ith port. In general, we use the tilde sign to denote a random variable, and boldface letters to denote the column vectors, for example, $\boldsymbol{x} = (x_1, x_2, \ldots, x_I)^T$.

We focus on a single round-trip voyage to obtain analytical insights. Let $\tilde{d}_i$ denote the arrival delay at the ith port of call. For tactical planning, it is reasonable to assume that a ship starts a round-trip voyage on time from its home port, i.e., $\tilde{d}_1 \equiv 0$. Nevertheless, our model is able to capture the reliability that the ship returns to the home port on time through η_{I+1}. Hence, by setting a high-reliability target for η_{I+1} and including the buffer time between two voyages into T, we can ensure with a high probability that the ship starts its next voyage on time. Define $\tilde{c}_i$ to be the difference between the actual inter arrival time and the scheduled interval time between the ith and $(i+1)^{\text{th}}$ port, i.e., $\tilde{c}_i = \tilde{\tau}_i + \tilde{\xi}_i - x_i$, $i = 1, 2, \ldots, I$. Then the arrival delay time at the ith port of call is given by

$$\begin{aligned} \tilde{d}_i &= \max\left\{0, \tilde{d}_{i-1} + \tilde{c}_{i-1}\right\} \\ &= \max\left\{0, \tilde{c}_{i-1}, \tilde{c}_{i-1} + \tilde{c}_{i-2}, \ldots, \sum_{k=1}^{i-1} \tilde{c}_k\right\}, \quad i = 2, 3, \ldots, I+1. \end{aligned} \tag{2}$$

The maximum partial sum formula shows the cascading effect of delays in earlier ports on the on-time arrival performance of the later parts of the voyage. The reliability target translates to choosing a timetable to ensure that $\mathbf{P}(\tilde{d}_i = 0) \geq \eta_i$ for all $i = 1, \ldots, I+1$. For given distribution $\tilde{c}_i$, the analysis of $\mathbf{P}(\tilde{d}_i = 0)$ is notoriously difficult and is a core challenge in the study of healthcare appointment system. We take a slightly different approach in this paper and use a distributionally robust model to analyze this problem in an implicit manner. While this is an inexact analysis, it allows us to perform the trade-offs

between T, B and the targets $\{\eta_i\}$ in a tractable manner.

More formally, to balance the delays at various parts of the voyages, we choose a surrogate objective to be minimizing the weighted sum of mean arrival delays, i.e., $\mathbf{E}[\sum_{i=2}^{I+1} w_i \tilde{d}_i]$, where w_i is the corresponding weight or the unit delay time cost at the ith port. Interestingly, we show later how the choice of w_i relates to the on-time probability target η_i.

Network Flow Model and Distributionally Robust Surrogate Schedule Reliability

The shipping network is depicted in Figure 3, where the container ship starts from the 1st port of call and sails to the 2nd one, and so on. The actual movement of the ship follows the solid lines. Note that a ship can visit the same port multiple times in a single route, but they are labeled with different indices in a sequence of port calls.
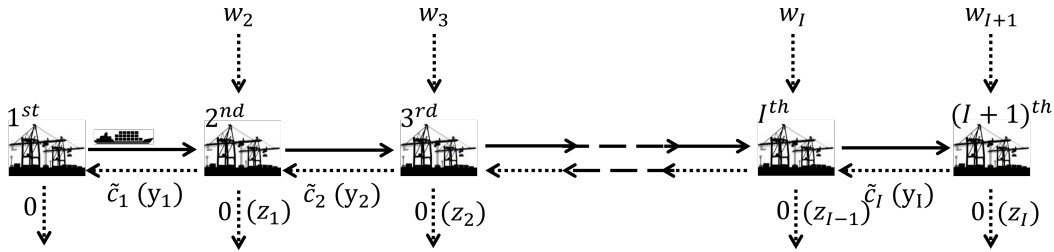

Figure 3: Shipping network

To capture the delay time, we construct a network flow model base on the shipping network such that the maximum cost flow equals the weighted sum of mean arrival delay. We first introduce reverse flows from the $(i+1)^{\text{th}}$ port to the ith port with cost $\tilde{c}_i$. The unit delay time cost w_i enters the network through the ith port as an incoming flow, and seeks the maximum cost path to exit the graph. Every incoming flow has the possibility to leave the network with zero cost (going down as in Figure 3), which represents the case of no delay at the ith port. The network flow arcs are represented with dotted lines in Figure 3. Numbers along the dotted lines represent the costs, and the symbols in brackets are flow variables. It can be easily verified against Equation (2) that the maximum cost flow of w_i is exactly the actual delay time at the ith port. For example, if a unit of flow enters the 3rd port, it will choose between the following three options to exit the network: 1) exit from the 3rd port immediately with a zero cost; 2) travel to the 2nd port and exit from there with a cost of $\tilde{c}_2$; 3) travel to the 2nd port first and then to the 1st port and exit from there with a cost of $\tilde{c}_2 + \tilde{c}_1$. Hence, the cost incurred by this unit of flow is $\max\{0, \tilde{c}_2, \tilde{c}_2 + \tilde{c}_1\}$, which is exactly the arrival delay at the 3rd port of call, $\tilde{d}_3$, as expressed in Equation (2).

With this construction, the optimal cost of the maximum cost flow problem on this network equals the weighted sum of mean delay times with given $\boldsymbol{x}$ and $\boldsymbol{v}$ under any realization of the uncertainties $\tilde{\boldsymbol{\tau}}$

12

and $\tilde{\boldsymbol{\epsilon}}$, denoted as $f(\boldsymbol{x}, \boldsymbol{v}, \tilde{\boldsymbol{\tau}}, \tilde{\boldsymbol{\epsilon}})$, i.e.,

$$
\begin{aligned}
f(\boldsymbol{x}, \boldsymbol{v}, \tilde{\boldsymbol{\tau}}, \tilde{\boldsymbol{\epsilon}}) \quad := \quad \max \quad & \sum_{i=1}^{I} \tilde{c}_i \cdot y_i = \sum_{i=1}^{I} \left(\tilde{\tau}_i + \frac{D_i}{v_i} + \tilde{\epsilon}_i - x_i \right) \cdot y_i \\
s.t. \quad & y_{i+1} - y_i - z_i = -w_{i+1}, \forall i = 1, 2, \ldots, I-1 \\
& -y_I - z_I = -w_{I+1} \\
& y_i, z_i \geq 0, \forall i = 1, 2, \ldots, I.
\end{aligned}
$$

We simplify the above optimization problem using matrix notation as follows:

$$
\begin{aligned}
f(\boldsymbol{x}, \boldsymbol{v}, \tilde{\boldsymbol{\tau}}, \tilde{\boldsymbol{\epsilon}}) \quad := \quad \max \quad & \tilde{\boldsymbol{c}}^T \boldsymbol{y} \\
s.t. \quad & \boldsymbol{a}_i^T \boldsymbol{y} - \boldsymbol{e}_i^T \boldsymbol{z} = -w_{i+1}, \forall i = 1, 2, \ldots I \\
& \boldsymbol{y}, \boldsymbol{z} \geq 0,
\end{aligned}
$$

where $\tilde{\boldsymbol{c}} = (\tilde{c}_1, \tilde{c}_2, \ldots, \tilde{c}_I)^T$, $\boldsymbol{y} = (y_1, y_2, \ldots, y_I)^T$, and $\boldsymbol{z} = (z_1, z_2, \ldots, z_I)^T$; and $\boldsymbol{e}_i \in \mathbb{R}^n$ is the unit vector with its ith entry being one; and $(\boldsymbol{a}_i)_i = -1$, for $i = 1, 2, \ldots I$, $(\boldsymbol{a}_i)_{i+1} = 1$, for $i = 1, 2, \ldots, I-1$, and $(\boldsymbol{a}_i)_k = 0$, otherwise.

As discussed before, we will apply the distributionally robust concept and solve for reliable schedule for the worst-case distribution, which means that we need to evaluate

$$
\sup_{\phi \in \Omega(\tilde{\boldsymbol{\tau}}, \tilde{\boldsymbol{\epsilon}})} \mathbf{E}_{\phi} \left[f(\boldsymbol{x}, \boldsymbol{v}, \tilde{\boldsymbol{\tau}}, \tilde{\boldsymbol{\epsilon}}) \right],
$$

where $\Omega(\tilde{\boldsymbol{\tau}}, \tilde{\boldsymbol{\epsilon}})$ is the set of joint distributions of $\tilde{\boldsymbol{\tau}}$ and $\tilde{\boldsymbol{\epsilon}}$, and $\mathbf{E}_{\phi}[\cdot]$ denotes that the expectation is taken over the distribution ϕ. The distributionally robust surrogate schedule reliability problem can be presented as

$$
(\text{P}) \qquad \min_{\boldsymbol{x}, \boldsymbol{v}} \sup_{\phi \in \Omega(\tilde{\boldsymbol{\tau}}, \tilde{\boldsymbol{\epsilon}})} \mathbf{E}_{\phi} \left[f(\boldsymbol{x}, \boldsymbol{v}, \tilde{\boldsymbol{\tau}}, \tilde{\boldsymbol{\epsilon}}) \right]
$$

Note that in $f(\boldsymbol{x}, \boldsymbol{v}, \tilde{\boldsymbol{\tau}}, \tilde{\boldsymbol{\epsilon}})$, $\tilde{\boldsymbol{\tau}}$ and $\tilde{\boldsymbol{\epsilon}}$ are linked to each other by summation in the objective. We show next that when $(\tilde{\boldsymbol{\tau}} + \tilde{\boldsymbol{\epsilon}})$ is characterized by the first two moments and nonnegative support, i.e.,

$$
\mathbf{E}\left[\tilde{\boldsymbol{\tau}} + \tilde{\boldsymbol{\epsilon}}\right] = \boldsymbol{\mu}, \ \mathbf{E}\left[(\tilde{\boldsymbol{\tau}} + \tilde{\boldsymbol{\epsilon}}) (\tilde{\boldsymbol{\tau}} + \tilde{\boldsymbol{\epsilon}})^T \right] = \Sigma, \ \mathbf{P}\left(\tilde{\boldsymbol{\tau}} + \tilde{\boldsymbol{\epsilon}} \geq 0\right) = 1,
$$

$\sup_{\phi \in \Omega(\tilde{\boldsymbol{\tau}}, \tilde{\boldsymbol{\epsilon}})} \mathbf{E}_{\phi}\left[f(\boldsymbol{x}, \boldsymbol{v}, \tilde{\boldsymbol{\tau}}, \tilde{\boldsymbol{\epsilon}}) \right]$ can be computed via a deterministic convex conic programming problem, under a mild technical assumption that $(1, \boldsymbol{\mu}, \Sigma)$ lies in the interior of the corresponding moment cone, which usually holds.

Proposition 1. *[Kong et al. (2013)] Let $u_i = 1/v_i$, $i = 1, 2, \ldots, I$. We have*

$$\sup_{\phi \in \Omega(\tilde{\boldsymbol{\tau}}, \tilde{\boldsymbol{\epsilon}})} \boldsymbol{E}_\phi \left[f\left(\boldsymbol{x}, \boldsymbol{v}, \tilde{\boldsymbol{\tau}}, \tilde{\boldsymbol{\epsilon}} \right) \right]$$

$$= \inf \Sigma \bullet \Gamma + \boldsymbol{\mu}^T \boldsymbol{\beta} + \theta$$

$$s.t. \quad \begin{pmatrix} \theta & \frac{\boldsymbol{\beta}^T}{2} & \frac{(\boldsymbol{x} - \boldsymbol{D} \circ \boldsymbol{u})^T}{2} & \boldsymbol{0}_{1 \times I} \\ \frac{\boldsymbol{\beta}}{2} & \Gamma & -\frac{\boldsymbol{I}_I}{2} & \boldsymbol{0}_{I \times I} \\ \frac{(\boldsymbol{x} - \boldsymbol{D} \circ \boldsymbol{u})}{2} & -\frac{\boldsymbol{I}_I}{2} & \boldsymbol{0}_{I \times I} & \boldsymbol{0}_{I \times I} \\ \boldsymbol{0}_{I \times 1} & \boldsymbol{0}_{I \times I} & \boldsymbol{0}_{I \times I} & \boldsymbol{0}_{I \times I} \end{pmatrix} + \sum_{i=1}^{I} \gamma_i \begin{pmatrix} w_{i+1} \\ \boldsymbol{0}_{I \times 1} \\ \boldsymbol{a}_i \\ -\boldsymbol{e}_i \end{pmatrix} \begin{pmatrix} w_{i+1} \\ \boldsymbol{0}_{I \times 1} \\ \boldsymbol{a}_i \\ -\boldsymbol{e}_i \end{pmatrix}^T \succeq_{co} 0,$$

where the decision variables are $\theta \in \mathbb{R}$, $\boldsymbol{\beta} \in \mathbb{R}^I$, $\Gamma \in \mathbb{R}^{I \times I}$, and $\boldsymbol{\gamma} \in \mathbb{R}^I$; $\boldsymbol{I}_n$ denotes an identity matrix of dimension $n \times n$; $\boldsymbol{0}_{m \times n}$ denotes a zero matrix of dimension $m \times n$; ($\bullet$) denotes the inner product; ($\circ$) denotes Hadamard product; and $A \succeq_{co} 0$ denotes that the symmetric matrix $A \in \mathbb{R}^{n \times n}$ is copositive, i.e., $\boldsymbol{v}^T A \boldsymbol{v} \geq 0$, for all $\boldsymbol{v} \in \mathbb{R}_+^n$.

The only constraint in the deterministic reformulation is a copositive cone constraint, which makes it a copositive program (COP)—i.e.,, the linear program over the cone of copositive matrices. The proof of this proposition is included in Appendix A for completeness. Proposition 1 gives a concise way to compute the worst-case weighted sum of the mean delay time of any given schedule and speed design. We build on this result to incorporate a conic reformulation of the budget bunker consumption constraint to reformulate Problem (P) into a deterministic convex optimization problem.

Theorem 2. *Let Π denote the space of all feasible schedules. The schedule that minimizes the worst-case weighted sum of mean delay time can be obtained by solving the following copositive program:*

$$(C) \quad \inf \quad \Sigma \bullet \Gamma + \boldsymbol{\mu}^T \boldsymbol{\beta} + \theta$$

$$s.t. \quad \begin{pmatrix} \theta & \frac{\boldsymbol{\beta}^T}{2} & \frac{(\boldsymbol{x} - \boldsymbol{D} \circ \boldsymbol{u})^T}{2} & \boldsymbol{0}_{1 \times I} \\ \frac{\boldsymbol{\beta}}{2} & \Gamma & -\frac{\boldsymbol{I}_I}{2} & \boldsymbol{0}_{I \times I} \\ \frac{(\boldsymbol{x} - \boldsymbol{D} \circ \boldsymbol{u})}{2} & -\frac{\boldsymbol{I}_I}{2} & \boldsymbol{0}_{I \times I} & \boldsymbol{0}_{I \times I} \\ \boldsymbol{0}_{I \times 1} & \boldsymbol{0}_{I \times I} & \boldsymbol{0}_{I \times I} & \boldsymbol{0}_{I \times I} \end{pmatrix} + \sum_{i=1}^{I} \gamma_i \begin{pmatrix} w_{i+1} \\ \boldsymbol{0}_{I \times 1} \\ \boldsymbol{a}(i) \\ -\boldsymbol{e}(i) \end{pmatrix} \begin{pmatrix} w_{i+1} \\ \boldsymbol{0}_{I \times 1} \\ \boldsymbol{a}(i) \\ -\boldsymbol{e}(i) \end{pmatrix}^T \succeq_{co} 0$$

$$\begin{pmatrix} g_i & h_i \\ h_i & 1 \end{pmatrix} \succeq 0, \forall i = 1, 2, \ldots, I$$

$$\begin{pmatrix} h_i - \frac{k_2}{2k_1} & 1 \\ 1 & u_i \end{pmatrix} \succeq 0, \forall i = 1, 2, \ldots, I$$

$$\sum_{i=1}^{I} D_i \left(k_1 g_i - \frac{k_2^2}{4k_1} + k_3 + k_4 u_i \right) \leq B$$

$$\frac{1}{v_i^{max}} \leq u_i \leq \frac{1}{v_i^{min}}, \forall i = 1, 2, \ldots, I$$

$$\boldsymbol{g}, \boldsymbol{h} \geq 0$$

$$\boldsymbol{x} \in \Pi$$

14

where the decision variables are $\theta \in \mathbb{R}$, $\boldsymbol{\beta} \in \mathbb{R}^{I}$, $\Gamma \in \mathbb{R}^{I \times I}$, $\boldsymbol{\gamma} \in \mathbb{R}^{I}$, $\boldsymbol{g} \in \mathbb{R}^{I}$, $\boldsymbol{h} \in \mathbb{R}^{I}$, $\boldsymbol{x} \in \mathbb{R}^{I}$ *and* $\boldsymbol{u} \in \mathbb{R}^{I}$; *and* $A \succeq 0$ *denotes that the symmetric matrix* $A \in \mathbb{R}^{n \times n}$ *is positive semidefinite.*

The proof of the above theorem is relegated to Appendix A. Note that the speed decisions are embedded in $\boldsymbol{u}$ by a simple variable transformation. As long as Π can be described by convex constraints on $\boldsymbol{x}$, we have a deterministic convex programming model to optimize the schedule under the stochastic environment. The two positive semidefinite constraints are essentially second order cone constraints. Typical constraints include nonnegativity and total voyage time constraints, i.e.,

$$\boldsymbol{x} \geq 0 \text{ and } \sum_{i=1}^{I} x_i \leq T. \tag{3}$$

Additional constraints will be discussed under respective numerical experiments in Section 5.

Remark 3. Note that although the service time, $\tilde{\boldsymbol{\tau}}$, is nonnegative, the sailing time noise, $\tilde{\boldsymbol{\epsilon}}$, can be negative. Consequently, the assumption that $\mathbf{P}\left(\tilde{\boldsymbol{\tau}} + \tilde{\boldsymbol{\epsilon}} \geq 0\right) = 1$ needs not hold. However, it is trivial to generalize the conic model to allow this assumption to be relaxed. Instead of requiring the matrix in Theorem 2 to be copositive, we restrict it to the space of $\left\{A \in \mathbb{R}^{(3I+1) \times (3I+1)} : \boldsymbol{v}^T A \boldsymbol{v} \geq 0, \forall \boldsymbol{v} \in \mathbb{R}_+ \times \mathbb{R} \times \mathbb{R}_+^{2I}\right\}$. The justification for this extension is included in the proof of Proposition (1) in Appendix A.

3.2 Schedule Reliability

Although our surrogate model captures the schedule reliability through minimizing expected delays, we show in this section that the on-time probability (or 1 - delay probability) is also reflected in our model, and we can take advantage of this to calibrate the model inputs, in particular, unit delay costs w_i.

Recall Figure 3, the flow entering the ith port can either leave the network or go to the $(i-1)^{\text{th}}$ port. The probability that the flow goes to the $(i-1)^{\text{th}}$ port is exactly the probability that the vessel is delayed to arrive at the ith port. Let $y_i^*\left(\boldsymbol{x}, \boldsymbol{v}, \tilde{\boldsymbol{\tau}}, \tilde{\boldsymbol{\epsilon}}\right)$ denote the optimal flow on the ith leg. From the above argument, we have

$$y_{i-1}^*\left(\boldsymbol{x}, \boldsymbol{v}, \tilde{\boldsymbol{\tau}}, \tilde{\boldsymbol{\epsilon}}\right) = \begin{cases} y_i^*\left(\boldsymbol{x}, \boldsymbol{v}, \tilde{\boldsymbol{\tau}}, \tilde{\boldsymbol{\epsilon}}\right) + w_i, & \text{if vessel is delayed to arrive at the } i^{th} \text{ port}, i = 2, 3, \dots, I, \\ 0, & \text{otherwise.} \end{cases}$$

Therefore, under any distribution of the uncertainties,

$$\begin{aligned} \mathbf{E}\left[y_{i-1}^*\left(\boldsymbol{x}, \boldsymbol{v}, \tilde{\boldsymbol{\tau}}, \tilde{\boldsymbol{\epsilon}}\right)\right] &= \mathbf{E}\left[\mathbf{E}\left[y_{i-1}^*\left(\boldsymbol{x}, \boldsymbol{v}, \tilde{\boldsymbol{\tau}}, \tilde{\boldsymbol{\epsilon}}\right) | y_i\left(\boldsymbol{x}, \boldsymbol{v}, \tilde{\boldsymbol{\tau}}, \tilde{\boldsymbol{\epsilon}}\right)\right]\right] \\ &= \left\{\mathbf{E}\left[y_i^*\left(\boldsymbol{x}, \boldsymbol{v}, \tilde{\boldsymbol{\tau}}, \tilde{\boldsymbol{\epsilon}}\right)\right] + w_i\right\} \mathbf{P}\left(\text{vessel is delayed to arrive at the } i^{th} \text{ port}\right), \end{aligned}$$

which gives an expression for the delay probability at the ith port:

$$\mathbf{P}\left(\text{vessel is delayed to arrive at the } i^{th} \text{ port}\right) = \frac{\mathbf{E}\left[y_{i-1}^*\left(\boldsymbol{x}, \boldsymbol{v}, \tilde{\boldsymbol{\tau}}, \tilde{\boldsymbol{\epsilon}}\right)\right]}{\mathbf{E}\left[y_i^*\left(\boldsymbol{x}, \boldsymbol{v}, \tilde{\boldsymbol{\tau}}, \tilde{\boldsymbol{\epsilon}}\right)\right] + w_i}, \ i = 2, 3, \ldots, I. \tag{4}$$

Similarly, we have the delay probability at the last port of call:

$$\mathbf{P}\left(\text{vessel is delayed to arrive at the last port}\right) = \frac{\mathbf{E}\left[y_I^*\left(\boldsymbol{x}, \boldsymbol{v}, \tilde{\boldsymbol{\tau}}, \tilde{\boldsymbol{\epsilon}}\right)\right]}{w_{I+1}}. \tag{5}$$

Suppose that the constraints for feasible schedules are captured in (3). By the KKT conditions, there exist dual multipliers such that:

$$\begin{cases} -\mathbf{E}_{\phi^*}\left[y_i^*\left(\boldsymbol{x}, \boldsymbol{v}, \tilde{\boldsymbol{\tau}}, \tilde{\boldsymbol{\epsilon}}\right)\right] + \lambda^* - \kappa_i^* = 0, \ \forall i = 1, 2, \ldots, I \\ \kappa_i^* x_i^* = 0, \ \forall i = 1, 2, \ldots, I \\ \lambda^* \geq 0 \end{cases}$$

where λ^* and κ_i^* are the dual variables of the total voyage time constraint and nonnegativity constraints of the schedule intervals, respectively, and ϕ^* denotes the worst-case distribution. The first KKT condition follows from the copositive cone constraint and decomposition analysis in Kong et al. (2013). Specifically, $\mathbf{E}_{\phi^*}[y_i^*(\boldsymbol{x}, \boldsymbol{v}, \tilde{\boldsymbol{\tau}}, \tilde{\boldsymbol{\epsilon}})]$ represent the dual variable of the copositive cone constraint in the $(1, I+1+i)$-entry, which is $(x_i - D_i u_i)/2$, $i = 1, 2 \ldots, I$.

Theoretically, it is possible that if the schedule is extremely tight, the optimal schedule may allocate zero interarrival times to some legs. However, this is impossible in practice since the total voyage time is usually determined first with a reasonable duration, and it does not make sense to publish a vessel schedule that announces to arrive at different ports at the same time, given the strictly positive sailing distance between any two ports. Therefore, we can safely assume that in an optimal solution, $x_i^* > 0$, for all i. Hence, $\kappa_i^* = 0$, and consequently, $\mathbf{E}_{\phi^*}[y_i^*(\boldsymbol{x}, \boldsymbol{v}, \tilde{\boldsymbol{\tau}}, \tilde{\boldsymbol{\epsilon}})] = \lambda^*$, for all i. This means the expected flows are equal to each other under the worst-case distribution as long as the scheduled vessel interarrival times are positive. We summarize this result below and then discuss how to use it to calibrate our model.

Proposition 4. *Suppose that the constraints for feasible schedules are characterized by* (3). *If in an optimal solution to Problem (C), the scheduled interarrival times are strictly positive, i.e., $x_i^* > 0$, $\forall i = 1, 2, \ldots, I$, then the network flow solution must satisfy $\boldsymbol{E}_{\phi^*}[y_i^*(\boldsymbol{x}, \boldsymbol{v}, \tilde{\boldsymbol{\tau}}, \tilde{\boldsymbol{\epsilon}})] = \lambda^*$, $\forall i = 1, 2, \ldots, I$.*

The next result follows immediately from Proposition 4 and Equations (4) and (5).

Corollary 5. *Suppose that the constraints for feasible schedules are captured in* (3). *If in an optimal solution to Problem (C), the scheduled vessel interarrival times are strictly positive, i.e., $x_i^* > 0$, $\forall i =$*

$1, 2, \ldots, I$, *then under the worst-case distribution and the optimal schedule from solving Problem (C),*

$$\boldsymbol{P}_{\phi^*} \left(vessel\ arrives\ late\ at\ the\ i^{th}\ port \right) = \frac{\lambda^*}{\lambda^* + w_i},\ i = 2, 3, \ldots, I,\ and \tag{6}$$

$$\boldsymbol{P}_{\phi^*} \left(vessel\ arrives\ late\ at\ the\ (last)\ (I+1)^{th}\ port \right) = \frac{\lambda^*}{w_{I+1}}. \tag{7}$$

Recall that λ^* is the optimal dual variable of the total voyage time constraint. When the total voyage time is sufficient, the marginal benefit from further increasing the total voyage time will be small, i.e., λ^* will be small, so the probabilities of delaying at each port will be small, which is intuitively true. When the total voyage time is tight, λ^* is non-negligible.

We discuss next how we can choose the weights based on the on-time probability targets $\{\eta_i : i = 2, \ldots I+1\}$. Note that the on-time arrival probability at the first port is always 100% under our modeling assumptions. Since the performance of the model does not change if we scale all the weights w_i's in the model by a common factor, we can set, without loss of generality, $w_{I+1} = 1$. Let $\hat{\eta}_i(\boldsymbol{w})$ denote the on-time arrival probability for our model using weight $\boldsymbol{w}$. Our approach relies on Corollary 5 to capture the relationship between the on-time arrival probability and the weights. To emphasize λ^*'s dependence on $\boldsymbol{w}$, we write $\lambda^*(\boldsymbol{w})$ in the following analysis.

From Corollary 5, we have:

$$w_i \frac{1 - \hat{\eta}_i(\boldsymbol{w})}{\hat{\eta}_i(\boldsymbol{w})} = \lambda^*(\boldsymbol{w}) = [1 - \hat{\eta}_{I+1}(\boldsymbol{w})] \overbrace{w_{I+1}}^{=1},\ i = 2, \ldots, I.$$

Therefore

$$w_i = [1 - \hat{\eta}_{I+1}(\boldsymbol{w})] \frac{\hat{\eta}_i(\boldsymbol{w})}{1 - \hat{\eta}_i(\boldsymbol{w})},\ i = 2, \ldots, I. \tag{8}$$

We want to choose a set of weights w_i so that $\hat{\eta}_i(\boldsymbol{w}) \geq \eta_i$, for all $i = 2, \ldots, I+1$. To achieve this, we first ignore the last condition. Next, we assume that the reliability targets are tight except for the last port, i.e., $\hat{\eta}_i(\boldsymbol{w}) = \eta_i$ for $i = 2, \ldots, I$. Then for any value of $\hat{\eta}_{I+1}(\boldsymbol{w})$, using Equation (8), we can choose the weight w_i for $i = 2, \ldots, I$, together with $w_{I+1} = 1$. We perform a binary search on the value of $\hat{\eta}_{I+1}(\boldsymbol{w})$ until $\lambda^*(\boldsymbol{w}) = 1 - \hat{\eta}_{I+1}(\boldsymbol{w})$. We can then check if the solution obtained satisfies $\hat{\eta}_{I+1}(\boldsymbol{w}) \geq \eta_{I+1}$. This reduces the schedule reliability problem to a one dimensional search problem on $\hat{\eta}_{I+1}(\boldsymbol{w})$. To see that a binary search is valid, note that $\lambda^*(\boldsymbol{w})$ is the optimal dual variable of the total voyage time constraint, so it is concave increasing in w_i. As w_i is decreasing linearly in $\bar{\eta}_{I+1}$, the output $\lambda^*(\boldsymbol{w})$ is then convex decreasing in $\bar{\eta}_{I+1}$. Moreover, when $\bar{\eta}_{I+1}$ is set to 1, $\lambda^*(\boldsymbol{w}) > 0 = 1 - \bar{\eta}_{I+1}$; when $\bar{\eta}_{I+1}$ is set to 0, $\lambda^*(\boldsymbol{w}) < 1 = 1 - \bar{\eta}_{I+1}$ as $\lambda^*(\boldsymbol{w})$ is bounded above by $w_{I+1} = 1$. Therefore, there exists a unique fixed point that can be checked via a binary search on $\bar{\eta}_{I+1}$. We state the algorithm formally as Schedule Reliability Algorithm (SRA) as follows:

Algorithm SRA.

INPUT: Service route, journey time T, bunker consumption budget B, and schedule reliability targets η_i, $i = 2, \ldots, I$.

OUTPUT: Achievable schedule reliability for the last port $\bar{\eta}_{I+1}$, and a feasible schedule (and sailing speeds) to achieve η_i for all $i = 2, \ldots, I$ and $\bar{\eta}_{I+1}$.

1. Conduct a binary search on $\bar{\eta}_{I+1} \in [0, 1]$ until $\lambda^*(\boldsymbol{w}) = 1 - \bar{\eta}_{I+1}$ through the following steps.

2. Initialize a value for $\bar{\eta}_{I+1}$, set $w_i = (1 - \bar{\eta}_{I+1})\frac{\eta_i}{1-\eta_i}$, $i = 2, \ldots I$, and $w_{I+1} = 1$.

3. Solve the convex relaxation to (C) to obtain $\lambda^*(\boldsymbol{w})$.

4. Check whether $|\lambda^*(\boldsymbol{w}) - (1 - \bar{\eta}_{I+1})| < \epsilon$, where $\epsilon > 0$ is a predefined precision parameter: if the inequality is met, terminate the algorithm, and output $\bar{\eta}_{I+1}$ and the schedule (including the sailing speeds); otherwise, continue the binary search and go to Step 2.

For a given bunker budget B, there is no guarantee that the weights chosen in this way (with fixed point $\bar{\eta}_{I+1}$) will necessarily lead to a good liner schedule, since $\bar{\eta}_{I+1}$ obtained could be low. Hence, there is a high probability that the vessel will not return to the first port on time to re-start the voyage. There is thus a fundamental trade-off between the right amount of bunker budget B and the reliability targets $\eta_2, \ldots, \eta_{I+1}$ that can be attained, assuming T fixed. This approach allows us to analyze this trade-off for given reliability targets, we can find the relationship between B and the fixed point $\bar{\eta}_{I+1}$, and choose B so that $\bar{\eta}_{I+1}$ is reasonably high to ensure that the next voyage can start on time with high probability. In this way, we obtain a fundamental relationship connecting the bunker budget with the reliability targets. This understanding is important to avoid the mistake of Daily Maersk, which probably aimed too high at on-time arrival targets, resulting in additional cost in bunker that cannot be fully offset by the market. We use Algorithm SRA to address the problem posed in the introduction.

Theorem 6. *Suppose the weight $\boldsymbol{w}$ is chosen by Algorithm SRA until $\lambda^*(\boldsymbol{w}) = 1 - \bar{\eta}_{I+1}$. If $\lambda^*(\boldsymbol{w}) \leq 1 - \eta_{I+1}$, then Problem (Q) is feasible, otherwise Problem (Q) is infeasible.*

The proof of the above theorem is given in Appendix A. With this result, we close the loop of analysis and address the fundamental question on how to design a timetable for a liner service that meets the given schedule reliability targets (if feasible) under a given bunker consumption budget, i.e., solving Problem (Q).

3.3 Optimal Speed

In this subsection, we also show that, if a shipping line has the freedom to choose its preferred berthing times at all ports, then the optimal speeds for all legs are identical under minor technical conditions

(typically satisfied in practice). Note that while we solve the schedule design problem using a convex approximation, we analyze the structural properties of the optimal speed in this subsection assuming an underlying distribution for the random parameters in the model, i.e., the results obtained here continue to hold and do not depend on the distributionally robust model used.

The schedule reliability performance is affected by the speed (and thus bunker consumed) of the vessel on each leg of the voyage. Given that the on-time arrival targets differ for different ports, it may seem natural for the vessel to traverse each leg with different speeds. We show next that surprisingly the optimal speed on each leg is identical in our model when the constraint on the schedule is characterized in (3) and the minimum and maximum speed constraints are not binding. In practice, the feasible range of the vessel speed is typically not limiting the liner schedule design. One of the key reasons is that the extreme speeds (either too fast or too slow) are harmful to the engine, and the liners tend to operate in a more conservative range compared to the hard limits (Maersk Line, 2011b). Suppose that the constraints for feasible schedules are again captured in (3). Under these conditions, our surrogate problem can be written as follows:

$$
\begin{aligned}
(\text{C}') \quad \min \quad & g\left(\frac{D_1}{v_1} - x_1, \frac{D_2}{v_2} - x_2, \ldots, \frac{D_N}{v_N} - x_N\right) \\
\text{s.t.} \quad & \sum_{i=1}^{I} D_i\left(k_1 v_i^2 + k_2 v_i + k_3 + \frac{k_4}{v_i}\right) \leq B \\
& \sum_{i=1}^{I} x_i \leq T, \; \boldsymbol{x} \geq 0
\end{aligned}
$$

where

$$
g\left(\frac{D_1}{v_1} - x_1, \frac{D_2}{v_2} - x_2, \ldots, \frac{D_N}{v_N} - x_N\right) := \sup_{\phi \in \Omega(\tilde{\boldsymbol{\tau}}, \tilde{\boldsymbol{\epsilon}})} \mathbf{E}_\phi\left[f\left(\boldsymbol{x}, \boldsymbol{v}, \tilde{\boldsymbol{\tau}}, \tilde{\boldsymbol{\epsilon}}\right)\right],
$$

is the second stage cost function, which is convex. Note that all the following analysis does not depend on the specific worst-case form of function $g()$. In fact, $g()$ can denote the expected weighted sum of delays under any specifically given distribution, and all the results continue to hold.

To show the identical speed result, we need the same technical condition used in the previous subsection that in an optimal solution, $x_i^* > 0$, for all i, which makes the dual variables of the nonnegativity constraints of the schedule intervals all equal to zero. Then we have the following KKT conditions:

$$
\begin{cases}
\frac{\partial}{\partial v_i} g\left(\frac{D_1}{v_1^*} - x_1^*, \ldots, \frac{D_N}{v_N^*} - x_N^*\right) & = \left. -\nu^* \frac{\partial}{\partial v_i}\left(D_i\left(k_1 v_i^2 + k_2 v_i + k_3 + \frac{k_4}{v_i}\right)\right)\right|_{v_i = v_i^*} \\
\frac{\partial}{\partial x_i} g\left(\frac{D_1}{v_1^*} - x_1^*, \ldots, \frac{D_N}{v_N^*} - x_N^*\right) & = -\lambda^*
\end{cases}
$$

where ν^* is the dual variable of the bunker consumption constraint, and λ^* is the dual variable of the total voyage time constraint as defined before. Hence, we have

$$
\begin{cases}
\left. \nabla g_i\left(\frac{D_1}{v_1^*} - x_1^*, \ldots, \frac{D_N}{v_N^*} - x_N^*\right) \frac{\partial}{\partial v_i}\left(\frac{D_i}{v_1} - x_i\right)\right|_{v_i = v_i^*, x_i = x_i^*} & = \left. -\nu^* \frac{\partial}{\partial v_i}\left(D_i\left(k_1 v_i^2 + k_2 v_i + k_3 + \frac{k_4}{v_i}\right)\right)\right|_{v_i = v_i^*} \\
\left. \nabla g_i\left(\frac{D_1}{v_1^*} - x_1^*, \ldots, \frac{D_N}{v_N^*} - x_N^*\right) \frac{\partial}{\partial x_i}\left(\frac{D_i}{v_i} - x_i\right)\right|_{v_i = v_i^*, x_i = x_i^*} & = -\lambda^*
\end{cases}
$$

19

which implies

$$\frac{\lambda^*}{(v_i^*)^2} = \nu^* \frac{\partial}{\partial v_i} \left(k_1 v_i^2 + k_2 v_i + k_3 + \frac{k_4}{v_i} \right) \Bigg|_{v_i = v_i^*}. \tag{9}$$

This establishes the next key result in the paper.

Theorem 7. *Suppose that the constraint on the schedule is characterized by (3) and a shipping line has the freedom to choose its preferred berthing times at all ports. If in an optimal solution to Problem (C), the scheduled interarrival times are strictly positive and minimum and maximum speed constraints are not binding, i.e., $x_i^* > 0$ and $v_i^{min} < v_i^* < v_i^{max}$, $\forall i = 1, 2, \ldots, I$, then the optimal speed in each leg, v_i^*, is identical for all legs.*

Theorem 7 suggests that the same nominal sailing speed at all sea legs is the most fuel-efficient for maximizing schedule reliability, which is in line with the finding of Lee et al. (2015) that it is always better to keep the speed constant to achieve the same navigation time. This theorem provides insight into what is preferred in setting sailing speeds. In reality, however, we need to acknowledge that it is often not feasible to design the same sailing speed at different legs due to operational constraints and commercial reasons. Liner ship timetable design has to consider the available berthing time windows at different ports, fixed start times for convoys at the Suez Canal, the presence of sulfur emission control areas, etc. Consequently, more often than not, the designed speeds are different at different legs, and they even can be different at different parts of the same leg. It is beyond the scope of this paper to analyze their effects as we focus on the structural properties of a most reliable schedule. Nevertheless, our model can be easily extended to capture practical considerations. For example, many shipping lines operate in tighter schedules for the headhaul route (e.g., from Asia to Europe for a service loop between Asia and Europe) than the backhaul route (e.g., from Europe to Asia). This is because the headhaul containers generate most of the revenue, and the shipping lines are under pressure to provide shippers fast delivery (Brouer et al., 2015). This requirement translates into an additional constraint on $\boldsymbol{x}$,

$$\sum_{i=1}^{H} x_i \leq T_H, \tag{10}$$

where H is the index of the last port of call in the headhaul route, and T_H is a given voyage time limit on the headhaul route. The above argument can be easily revised to incorporate the dual variable of constraint (10). Consequently, Theorem 7 can be adapted to the following corollary.

Corollary 8. *Suppose that the constraint on the schedule is characterized by (3) and (10). If in an optimal solution to Problem (C), the scheduled interarrival times are strictly positive and minimum and maximum speed constraints are not binding, i.e., $x_i^* > 0$ and $v_i^{min} < v_i^* < v_i^{max}$, $\forall i = 1, 2, \ldots, I$, then the optimal speed for each leg in the headhaul route is identical, and the optimal speed for each leg in the*

backhaul route is also identical. The headhaul speed is higher than or equal to the backhaul speed, and the equality holds when the headhaul voyage time constraint is not binding at the optimal solution.

The last conclusion in the above corollary follows directly from the fact that the dual variable of the headhaul voyage time constraint is nonnegative, and the complementarity condition implies that the dual variable is zero when the constraint is not binding. This result reflects a common practice in the industry that shipping lines usually set backhaul speed several knots slower than headhaul speed to save bunker (Brouer et al., 2015).

It is worthwhile noting that a similar optimal identical sailing speed result was shown in Wang et al. (2013) in a very different model, whose objective function is to minimize the bunker cost that is linear in the bunker consumption function. Their bunker consumption function is assumed to be strictly convex and non-decreasing in the sailing speed, and the model does not consider scheduling decisions or any uncertainties. When there are no time window restrictions, the optimal identical sailing speed follows from the convexity of the objective function. Our results extend such conclusion and confirm that the identical sailing speed is still optimal in a more complex environment, in which both the schedule and speeds are optimized simultaneously to minimize the expected weighted sum of delay times with uncertain port and sea times, and the bunker consumption is cubic in sailing speed.

4   Model Extensions

In this section, we develop several extensions of our model to capture more realistic and complicated scheduling scenarios. Specifically, we consider the uncertainty in bunker price, the schedule reliability of a network of fleets, and nonidentical bunker consumption functions at different legs.

4.1   Bunker Cost Uncertainty

In our model, we impose a fixed bunker consumption budget for the entire voyage. This parameter plays a key role in the design of a reliable schedule. However, in practice, the price of the bunker often affects the total amount of bunker the shipping line can consume. For instance, Figure 4 shows how the prices for different classes of fuel oil fluctuate in Singapore over the last six months in 2019–2020. This affects the speed the vessel will opt to sail in, and thus will affect the schedule reliability of the liner.

When the conditions for Theorem 7 hold, we can incorporate this source of uncertainty into our model without any side complication, if in an optimal solution to Problem (C), the scheduled interarrival times are strictly positive and minimum and maximum speed constraints are not binding. To see this, observe that in the optimal solution, for any fixed bunker consumption budget B, the optimal constant speed v^*
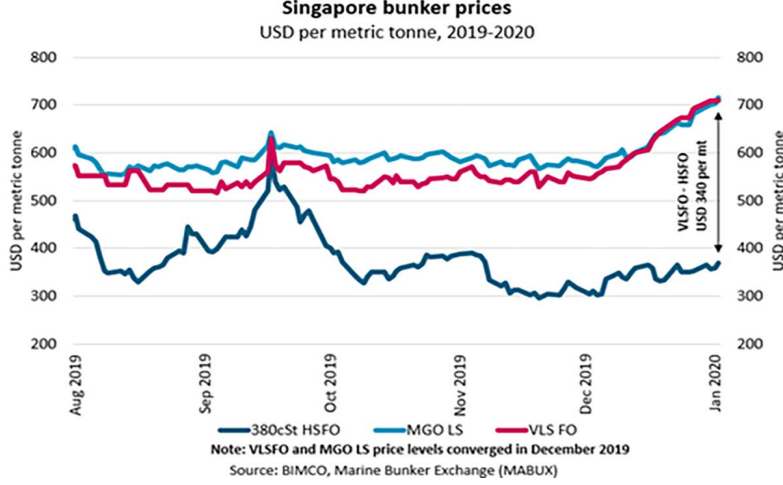
Figure 4: Singapore Bunker prices in 2019-2020

can be obtained by solving the following equation:

$$\sum_{i=1}^{I} D_i \left(k_1 (v^*)^2 + k_2 v^* + k_3 + \frac{k_4}{v^*} \right) = B.$$

In other words, v^* can be viewed as a function of the given bunker consumption budget B, i.e., $v^*(B)$. To capture the uncertainty in bunker budget, we replace B in the above equation by an uncertain budget $\tilde{B} := b(\tilde{p})$, where $b()$ is a function of the random bunker price index $\tilde{p}$. Hence the common speed $v^*(\tilde{B})$ satisfies

$$k_1 v^*(\tilde{B})^2 + k_2 v^*(\tilde{B}) + k_3 + \frac{k_4}{v^*(\tilde{B})} = \frac{\tilde{B}}{\sum\limits_{i=1}^{I} D_i}. \tag{11}$$

We use this relationship to incorporate the uncertainty in $\tilde{B}$ into our formulation by solving the following problem:

$$(P^B) \qquad \min_{\boldsymbol{x}} \ \sup_{\phi \in \Omega\left(\tilde{\boldsymbol{\tau}}, \tilde{\boldsymbol{\epsilon}}, \tilde{B}\right)} \ \mathbf{E}_\phi \left[f\left(\boldsymbol{x}, \tilde{B}, \tilde{\boldsymbol{\tau}}, \tilde{\boldsymbol{\epsilon}} \right) \right]$$

where

$$
\begin{aligned}
f\left(\boldsymbol{x}, \tilde{B}, \tilde{\boldsymbol{\tau}}, \tilde{\boldsymbol{\epsilon}} \right) \quad := \quad \max \quad & \sum_{i=1}^{I} \tilde{c}_i \cdot y_i = \sum_{i=1}^{I} \left(\tilde{\tau}_i + \frac{D_i}{v^*(\tilde{B})} + \tilde{\epsilon}_i - x_i \right) \cdot y_i \\
s.t. \quad & y_{i+1} - y_i - z_i = -w_{i+1}, \ \forall i = 1, 2, \dots, I-1 \\
& -y_I - z_I = -w_{I+1} \\
& y_i, z_i \geq 0, \ \forall i = 1, 2, \dots, I.
\end{aligned}
$$

The moment cone is now determined by the random parameters $\tilde{\tau}_i + \frac{D_i}{v^*(\tilde{B})} + \tilde{\epsilon}_i$, and the input moment information can be obtained by simply simulating the empirical distribution of $\tilde{B}$ based on the historical data. We state this formally in the next theorem.

22

Theorem 9. *In the case that the conditions for Theorem 7 holds, the liner timetable design problem, with random bunker budget $\tilde{B}$ and weights $\boldsymbol{w}$, can be solved as a distributionally robust appointment scheduling problem (P^B), where the appointment duration has distribution $\tilde{\tau}_i + \frac{D_i}{v^*(\tilde{B})} + \tilde{\epsilon}_i$, and $v^*(\tilde{B})$ is a solution to Equation (11).*

4.2 Multiple Services

A liner shipping network contains several liner services that are connected at different ports. Transshipment imposes huge complexity in optimizing the schedule reliability for a liner shipping network. In many cases, the schedule reliability of a service is often affected by the reliability of its connecting services, and vice versa. For instance, Figure 5 shows a network consisting of three liner services, which are connected to different markets. The port Tangier is a transshipment hub where cargo is transshipped from one service to another.
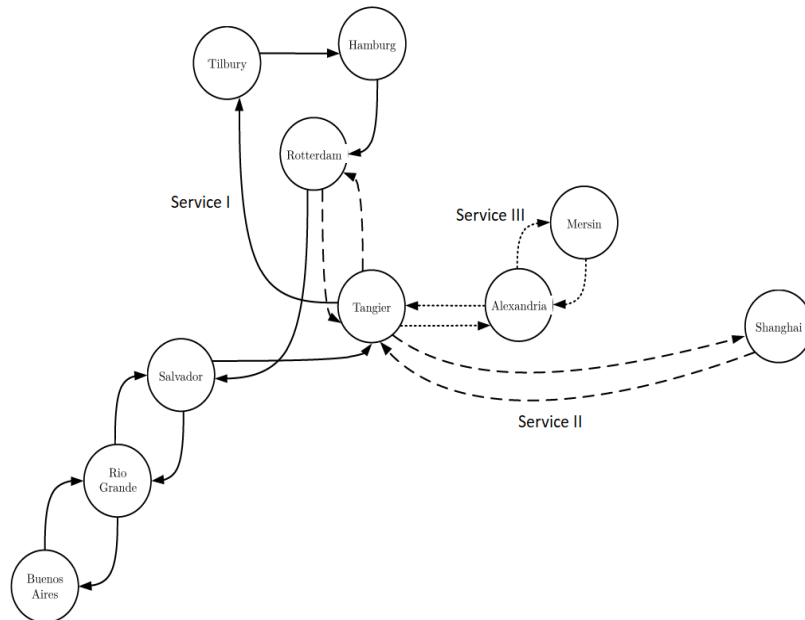

Figure 5: Network schedule reliability

Strictly speaking, once the timetable of a liner service is fixed, the vessel should try to follow the timetable and the reliability of other services should not affect the departure decision of the vessel at a port. However, in practice, a liner service may sometimes want to wait for connecting services to bring containers to the transshipment hubs depending on the business arrangements with collaborating liner services. To help make such decisions, the shipping company needs to know the on-time probability of transshipment containers. Therefore, we develop this extension based on our model to design and analyze the schedule reliability of the liner network.

As an illustration, we view the transshipment service at port Tangier where containers are transhipped from Services II and III to Service I, the main service. Specifically, we consider containers sent from

Shanghai to Tangier (transshipped at Tangier) to Tilbury and from Alexandria to Tangier (transshipped at Tangier) to Tilbury. By a slight abuse of notation, let $\eta^J_{A,B}$ be the on-time arrival target for service J in the leg from port A to B, in the design of the liner schedule for service J using our model. In this case, due to transshipment activities at port Tangier, the reliability of service I is affected by the on-time arrival performance of both service II in the leg from Shanghai to Tangier, and also service III in the leg from Alexandria to Tangier. Assuming that the on-time arrival probabilities for both services are independent, then the on-time probability of transshipment containers being ready for service I is given by $\eta^{II}_{Shanghai, Tangier} \times \eta^{III}_{Alexandria, Tangier}$. If a mainline vessel decides to wait at port Tangier for transshipment containers from services II and III, the port time for service I at port Tangier is a random function of the reliability targets $\eta^{II}_{Shanghai, Tangier}$ and $\eta^{III}_{Alexandria, Tangier}$. By varying the choices of the reliability targets for individual services, the shipping company can control the schedule reliability of its transshipment service in timetable design. Following the same logic, we can also extend the model to capture additional transshipment from Rotterdam to Tangier (transshipped at Tangier) to Tilbury. However, in calibrating the model, we need to consider the correlation between the schedule reliability between $\eta^{II}_{Shanghai, Tangier}$ and $\eta^{II}_{Rotterdam, Tangier}$. Nevertheless, one can either assume independence—which is likely to give a conservative lower bound since they are from the same service and the delay at earlier ports can propagate to later ports—or use simulation to calibrate the port time.

4.3 Nonidentical Bunker Consumption Functions

In the base model, we use an identical bunker consumption function for all legs. In reality, however, the consumption functions could be different in different legs because of distinct geographic conditions such as sea currents, waves, route layout, etc., in these legs. We can extend our model to capture nonidentical bunker consumption functions for different legs. In particular, the bunker consumption budget constraint can be extended to the following:

$$\sum_{i=1}^{I} \frac{D_i}{v_i} \left(k_{i,1} v_i^3 + k_{i,2} v_i^2 + k_{i,3} v_i + k_{i,4} \right) \leq B, \tag{12}$$

where $k_{i,1}$, $k_{i,2}$, $k_{i,3}$ and $k_{i,4}$ are constants used to characterize the bunker consumption functions for the ith leg, $i = 1, 2, \ldots, I$.

The reformulation result, i.e., Theorem 2, will continue to hold with a slight modification of changing the parameters k_j to $k_{i,j}$ for $i = 1, 2, \ldots, I$ and $j = 1, 2, 3, 4$. Hence, we can solve a convex optimization model to obtain the solution to the surrogate problem. Moreover, the results in Section 3.2 will also hold, and we can still use Algorithm SRA to find an optimal schedule that achieves the reliability targets. Therefore, when there are sufficient data to calibrate bunker consumption functions for different vessels at different legs, we can deploy the extended model to design the schedule to achieve the target reliability

at a given bunker consumption budget. However, the optimal constant speed result in Theorem 7 will not hold universally for all legs. From the proof, we can see that the optimal speeds for two legs will be identical only when the bunker consumption functions for these two legs are the same.

5   Numerical Experiments

This section validates the approach presented in the previous sections via simulation experiments. We first use the COP model to incorporate schedule reliability targets at some hub ports in schedule design. The numerical experiments lead to the discovery of a simple but very effective tactic in schedule design for guarding the service reliability at hub ports. We then benchmark the performance of the COP schedule against a former Daily Maersk service between Asia and Europe, AE2. As mentioned earlier, the now-abandoned Daily Maersk product achieved the best (over 98%) schedule reliability in liner shipping. Lastly, we compare the performance of the COP model with a heuristic that is widely used by shipping lines for schedule design. The COP schedules outperform the heuristic in schedule reliability and fuel efficiency. Our results also suggest that beyond a certain threshold on schedule reliability, a large amount of bunker needs to be consumed to improve the reliability by a small amount, indicating that absolute reliability is probably too costly a goal in this problem.

The machine used to conduct the numerical studies is HP Elitebook with Intel Core i5-8365U CPU 1.90 GHz, RAM 16GB, Microsoft Windows 10 Enterprise. MOSEK 9.2 is used to solve the doubly nonnegative approximation of the COP programs in MATLAB R2017a environment with YALMIP as the user interface (Lofberg, 2004). All the problem instances are solved within 10 seconds. Although we are not solving the COP programs exactly, the performance from the approximation is already quite good from our simulations.

5.1   Case Data

We obtained about 11,000 Daily Maersk port times between mid-2012 and early-2015 from the Maersk Line. After some analysis, we decided to use only about 1,200 port times for the period from mid-2012 to mid-2013, during which no major changes were made to the AE2 service. This was to ensure all port times are comparable. During the period, AE2 called at 19 ports, and its total voyage time for a round trip was 11 weeks. Most of the deployed vessels had a carrying capacity of 8,400 twenty-foot equivalent units (TEUs). Note that vessel size has a direct impact on port time and schedule design. A larger vessel usually stays longer in a port for container unloading/loading due to the increased carrying capacity. Starting from the mid-2013, Maersk Line started to upscale AE2 vessels to those of a carrying capacity of 13,000/15,500 TEUs, and then to Triple-E vessels (18,340 TEUs) in late 2014. To accommodate the longer port stays, consequently, the number of port calls has been reduced to 13 at the time of this paper.

The values of coefficients in the bunker consumption function as defined in constraint (1) are given as follows: $k_1 = 0.0036$, $k_2 = -0.1015$, $k_3 = 0.8848$, and $k_4 = 0$ (Fagerholt et al., 2010). The feasible speed interval is set from 14 to 25 knots.

Sailing time noises ($\tilde{\epsilon}_i$) are estimated based on the sea contingency times. Sea contingency times are the additional times allocated on top of the expected sailing times. Many shipping lines allocate sea contingency times in the service schedules to buffer against uncertainties at sea (Wang & Meng, 2012b). Based on the information from industry professionals, we set sea contingency time as 1 hour per 100 nautical miles (nm) for a distance of up to 1,000 nm with 1 hour being the minimum. For the distance between 1,000 and 4,000 nm, 1 hour sea contingency time is allocated per 200 nm, with 25 hours being the maximum. Sea contingency time is usually sufficient to buffer against random noises in sailings but not extreme weather conditions. No data is directly available about sailing delays in liner shipping, partly due to the complexity of sailing operations. We estimate sailing time delay means and variances by assuming that they follow half-normal distributions, and their standard deviations are equal to the corresponding sea contingency times, i.e., about 65% of the sailing delays fall within the one sigma control limits that are equal to the sea contingency times. It is reasonable to assume that the sailing time noises are independent of the stochastic service time at the ports (i.e., port times, $\tilde{\tau}_i$), which are typically resulted from operational uncertainties. Therefore, we can sum up the moments of the sailing time noises and port times to get the values for $\boldsymbol{\mu}$ and Σ. A summary of the data used for the numerical experiments is provided in Table 1 in Appendix B.

5.2 Incorporating Schedule Reliability Targets in Schedule Design

This subsection employs the COP model to incorporate schedule reliability targets in schedule design. We pay special attention to schedule reliability at hub ports because they are playing an increasingly important role in global container trade as the volume of containers being transshipped at hub ports continues to rise. A hub port's schedule reliability heavily affects a carrier's global schedule reliability because delays at a hub have a ripple effect in the whole service network. This explains why Maersk Line, as an industry leader in schedule reliability, actively manages schedule reliability at its global hub terminals. In fact, its sister company, APM Terminals, strategically owns and operates many of its hub terminals to ensure the best control of services at the hubs. Hub port schedule reliability is also named as spine reliability by Maersk Line because the hub ports form the spine of its service networks.

We demonstrate the effectiveness of our modeling approach by using the parameters as provided in Table 1. We single out two major hubs of the Maersk Line: Tanjung Pelepas and Rotterdam. We consider a 11-week service with a bunker budget of 7,375 tons. Recall that η_{I+1} refers to the reliability target at returning to the home port. Let η_h denote the reliability target at the two hub ports and η_n the reliability target at all other ports. We consider three sets of schedule reliability targets: Target

Set I: $\eta_n = \eta_h = 0.4$; Target Set II: $\eta_n = 0.4$, $\eta_h = 0.6$; Target Set III: $\eta_n = 0.4$, $\eta_h = 0.8$. Following Algorithm SRA proposed in Section 3.2, we derive the achievable reliability target for η_{I+1}. Specifically, $\eta_{I+1} = 0.7925, 0.7425$, and 0.539 for the three target sets.

In all the problem instances, the COP model sets a same sailing speed of 20 knots at all legs. This affirms that the most reliable schedule requires equal sailing speeds at all legs as established in Theorem 4 in the preceding section. From a planning perspective, once a shipping line fixes a bunker budget for a service, the default sailing speed is determined. We build a simulation model (Simulation A) in MATLAB to compare the performance of the schedules. The simulation sets a fixed sailing speed based on the designed sailing speeds, i.e., the vessel will not speed up or slow down based on the realized uncertainties in the past. In the simulations, delay time at the first port is zero because a vessel always starts a journey on time. We first calculate schedule reliability by giving no delay allowance to vessel arrivals when determining whether they are late[4]. This allows us to compare the actual performance outcomes with the reliability targets set according to the theoretical analysis presented in Section 3.2. We also report schedule reliability results based on the standard of Maersk Line, which gives a delay allowance of 12 hours. The simulation experiments evaluate four common (uniform, normal, Gamma and two-point) distribution types for stochastic port times and sailing delays, assuming the same first and second moment values as given in Table 1. We conduct 50,000 simulation runs for each distribution type.

The detailed reliability performance of three COP schedules are given in Table 2 in Appendix B. The simulation results show that arrivals at almost all ports including the hub ports meet the reliability targets when there is zero delay allowance. The few exceptions were only slightly below the targets. This is understandable due to the nature of approximation used in the solution method. When there is a delay allowance of 12 hours, the schedule reliability figures are obviously higher, which is no surprise. Overall the Algorithm SRA is effective for calibrating the weights in the COP model to help design service schedules that achieve realistic reliability targets at port calls.

These results shed light on the impact of the calibrated weights on the COP schedules and their reliability performance. In comparison with the Schedule I, the Schedule II achieves higher reliability performance at the two hub ports by assigning them a higher weight. The reliability performance at the two hubs is further improved by assigning them a greater weight in the Schedule III. However, when the reliability at the hub ports increases, the probability of returning to the home port on time is reduced and the trade-off is reasonable. The key observation from comparing the schedules is more buffer time being allocated to the schedule intervals right before the hub ports to achieve a higher reliability target. For example, the schedule interval between Le Havre and Rotterdam increases from 37.1 hours as in the Schedule I to 42.2 hours as in the Schedule II, and then further to 54.5 hours as in the Schedule III.

---

[4]The industry reports typically allow for six to twenty-four hours of delays in their computation of on-time arrival statistics.

Allocating more time to this particular schedule interval buffers against the potential delays in arriving at Rotterdam which may be accumulated at all the preceding schedule intervals.

To capture more realistic speed adjustments at sea, we build another simulation model (Simulation B). This simulation model allows a vessel to sail at a speed that is different from the designed sailing speed. When a vessel departs from a port, the captain sets a fixed sailing speed to arrive just on time at the next port (Aydin et al., 2017). We assume the captain is experienced and has sufficient weather information for the immediate sailing to the next port. This is not a strong assumption given the advanced technologies employed for the weather forecast. In reality, the captain may not always keep the same sailing speed in a leg, depending on the situation at sea. Still, he has an economic incentive to do so to minimize bunker consumption (Lee et al., 2015). As mentioned in 3.1, a vessel arrives at a port early has to wait for its scheduled time window (Qi & Song, 2012). If a vessel leaves a port early, it adopts a lower speed to save bunker, subject to the minimal vessel speed constraint. However, if a vessel leaves a port late, it speeds up to recover time loss but its speed does not exceed the "planned maximum sailing speed" (Song et al., 2015). A shipping line's planned maximum sailing speed is usually well below the maximum vessel speed to control bunker consumption. According to our knowledge, in the industry, the planned maximum speed is often the default steaming speed for timetable planning purposes. In real time, vessel speed is dynamically adjusted between the minimum vessel speed and planned maximum speed depending on the realizations of uncertain time parameters (Song et al., 2015; Aydin et al., 2017). Let v^{min} denote the minimum vessel speed and v^p denote the planned maximum speed, the rules for setting the speed at each leg can be defined as follows:

$$v_i = \max\left\{v^{min}, \min\left\{v^p, \frac{D_i}{x_i - \tilde{d}_i - \tilde{\tau}_i - \tilde{\epsilon}_i}\right\}\right\},$$

where D_i is the sailing distance of the ith leg as defined in section 3; $\tilde{\tau}_i$ denotes the stochastic service time at the the ith port; $\tilde{\epsilon}_i$ represents the noise in the sailing time due to external conditions; x_i is the scheduled arrival time interval between the ith and $(i + 1)^{\text{th}}$ port; and $\tilde{d}_i$ denotes the arrival delay at the ith port of call. The second term in the min operator, $D_i/(x_i - \tilde{d}_i - \tilde{\tau}_i - \tilde{\epsilon}_i)$, denotes the speed required to reach the next port exactly on time given the delay in the current port and a perfect forecast of sailing time uncertainty to the next port. However, this speed is not always feasible, and the min and max operators make sure that the actual sailing speed is between the minimum speed and the planned maximum speed.

For illustration purposes, we set the minimum sailing speed as 15 knots and the planned maximum speed as 22 knots, which is 2 knots higher than the default sailing speed of the COP schedules. We run simulation 50,000 times for Schedule II to observe the effect of dynamic speed adjustments between the minimum vessel speed and planned maximum speed. The results on schedule reliability are presented

in Table 3 in Appendix B. In comparison with fixing the sailing speed at 20 knots at all legs, allowing a vessel to speed up to 22 knots for schedule recovery increases the average reliability from 90.3% to 96.3%. More interestingly, the average bunker consumption is reduced from 7,375 tons to 6,588 tons. This finding is similar to that of Aydin et al. (2017): in comparison with a deterministic scenario, bunker consumption can be reduced substantially if dynamic speed decisions are made considering the uncertainty of port times. This is because the increased bunker consumption for speeding up at some legs is offset by the reduced bunker consumption in other legs when a vessel can slow down to as slow as 15 knots, the minimum vessel speed. This may not always be achievable in practice because a vessel may need to sail at a slightly higher speed to arrive early at the next port to avoid missing the scheduled time window, given that it is unlikely to have perfect information about the uncertain sailing delays at sea. However, the simulation results still clearly affirm the common practice of dynamic speed adjustments in liner shipping because it is beneficial for saving bunker while at the same time improving service reliability.

Besides speeding up, the other possible schedule recovery strategy is to skip one or more ports of call (Mulder & Dekker, 2019). We extend Simulation B to Simulation C to investigate its effect on service reliability. Similar to the work of Mulder & Dekker (2019), we consider multiple ports of call that could be skipped. For the concerned AE2 service, they are Xingang, Hamburg, and Felixstowe ports. Visiting these ports requires a detour from the main route, so skipping them can reduce sailing distance, allowing the vessel to catch up the schedule to the following ports. They are also not too far from another AE2 port of call, so it is relatively less costly to organize feeders or landside transport to redirect containers from or destined for these ports in case they are skipped. We assume that when a vessel arrives at a preceding port of one of these three ports, the captain decides whether the next port of call will be skipped based on the accumulated delay of arrival at the current port. If the delay is more than 48 hours, the next port of call will be skipped.

Table 4 in Appendix B shows the simulation results when both speeding up and port skipping can be used for schedule recovery. Out of 5,000 simulation runs, Hamburg and Felixstowe are skipped 8 and 10 times, respectively. The frequency of port skipping is affected by the distribution type of uncertain time parameters. For all the 18 times of port skipping, 14 of them are triggered under the Gamma distribution type. This suggests that big delays are more likely to occur when the uncertain time parameters obey a Gamma distribution, assuming their first and second moment values are the same. With schedule recovery by port skipping, service reliability at the next port is better protected. However, given that port skipping is rare, it does not significantly impact the overall service reliability. Note that port skipping is very disruptive to cargo operations because the containers destined to a skipped port have to be discharged at a different port. Consequently, it makes a big change in transport planning to get them to their final destinations. Therefore, port skipping is practiced only when there is a big delay, mainly

due to a disruptive event. In fact, there was no single port-skipping event in our data set for the AE2 service. The impact of a disruptive event is best managed at operational-level planning, while regular uncertainties are managed at tactical level planning (Li et al., 2016).

5.3 Daily Maersk Schedule Comparison

This subsection compares the performance of our COP schedule with the actual AE2 schedule. We first set COP model parameters comparable to those of AE2. We run the Simulation B 50,000 times for each distribution type to simulate AE2's bunker consumption and on-time arrival probability. Given Daily Maersk's commitment to absolute reliability, we set its planned maximum speed equal to the maximum vessel speed, 25 knots. It is observed that the worst-case bunker consumption is 12,335 tons, which occurs in one scenario under the normal distribution. Therefore, we set the bunker limit for our model as 12,335 tons for a fair comparison. The worst-case reliability under zero delay allowance is 81.14% at Rotterdam and Bremerhaven, the two AE2 European ports which were covered by Daily Maersk's promise of absolute reliability. Given the nature of the COP model being a distributionally robust optimization program, we set the reliability targets η_i according to this number.

To ensure the performance of the COP schedule is comparable to the Daily Maersk service, we impose the following two transit time constraints between Ningbo and Rotterdam, and between Ningbo and Bremerhaven, by following the Daily Maersk's transit time promise. The Daily Maersk product used multiple intercontinental services, including AE2 and many regional feeder services, to deliver its transit time promise between Asia and North Europe. It is beyond the scope of this paper to go into the details of how Maersk Line organized many services to make up the Daily Maersk product.

$$\sum_{i=6}^{12} x_i \leq 702, \sum_{i=6}^{13} x_i \leq 769$$

By following the Algorithm SRA, we generate the optimal COP schedule when the binary search of η_{I+1} converges at 95.35%. The weight w_i is derived as 0.20 and w_{I+1} is fixed as 1.

The COP program performs surprisingly well as its optimal schedule closely resembles the actual Maersk schedule whose reliability performance was outstanding. Detailed schedules and optimal speeds from our COP model are provided in Table 5 in Appendix B. For all the 19 legs included in the service route, the biggest schedule difference is only 20.5 hours. This is exceptional in light of the fact that a widely used standard in the liner shipping industry considers only a delay of more than 24 hours as lateness (Drewry, 2013). The COP model sets a lower designed speed of 22.8 knots from Rotterdam to Ningbo, but a higher speed of 24.5 knots from Ningbo to Rotterdam, in order to meet the Daily Maersk transit time requirements. For each of these two parts of the voyage, the speeds at all legs are identical, which affirms the Corollary 8 established in the preceding section.

Detailed simulation results are presented in Tables 6 and 7 in Appendix B. Following the standard of Maersk Line, a delay of fewer than 12 hours is not regarded as lateness. Therefore, the reported on-time probabilities in Tables 6 and 7 incorporate this allowance of 12 hours. Note that the 88.14% target used in deriving the COP schedule is obtained under zero delay allowance, which is in line with our surrogate model. The AE2 schedule achieves an average on-time probability of 98.3% (delay time average of 0.62 hours), with a range of 24.9% considering all ports across four distribution types. This result is in line with the actual performance of Daily Maersk, which achieved over 98% schedule reliability in practice. However, our simulations suggest that the COP schedule can further improve the average on-time probability to 99.6% (delay time average of 0.36 hours), with a range of 3.5% only. We can observe that the Daily Maersk schedule achieves a quite unbalanced reliability performance with almost 100% reliability in many ports but very poor performance in a few ports. In contrast, the COP schedule balances the reliability performance in all ports with negligible sacrifice in the reliability of those ports that achieve almost 100% reliability under the Maersk schedule. It is apparent that uncertain time parameters' distributions only have a marginal effect on the reliability performance of the COP schedule. This affirms that the COP modeling approach is indeed distributionally robust. More importantly, the bunker consumption of the COP schedule is 7,952 tons on average across four distributions, which is 11.4% lower than that of the AE2 schedule (8,979 tons). This demonstrates the advantage of our model in balancing the trade-off between schedule reliability and bunker consumption.

We also run Simulation C to allow schedule recovery by port skipping. However, no port is skipped in 5,000 simulation runs. This is understandable because of the very high schedule reliability at all ports of call. Therefore, there is no arrival delay of more than 48 hours at any port, which is required for triggering a port skipping decision.

5.4 Heuristic Schedule Comparison and the Cost of Absolute Reliability

This subsection compares the performance of the COP program with a heuristic that is widely used in the liner shipping industry for schedule design. When a shipping line designs a service route, the total voyage time and planned maximum speed are important decisions to be made together with port rotation (Song et al., 2015). From the perspective of shippers, the total voyage time largely determines port to port transit time, which has direct implications for door-to-door transportation lead time and supply chain inventories (Zhang & Lam, 2015). For shipping lines, they are highly concerned about bunker cost, which is often the largest cost component in maritime transport. At the schedule design stage, shipping lines set a fixed sailing speed at a leg because it leads to lower bunker consumption than a variable speed for covering the same distance (Lee et al., 2015). As mentioned earlier, when a vessel is on a voyage, its speed is dynamically adjusted between the minimum vessel speed and planned maximum speed depending on the realizations of uncertain time parameters (Song et al., 2015). When facing delays

at sea or a port, a vessel may sail at the planned maximum speed but usually not faster. Part of the reason is that it is costly to sail at a higher speed, and they do not have any model to quantify the associated benefits of making a delivery on time (Lee et al., 2015). Even if they do sail faster to improve delivery reliability, shippers are not willing to pay for a higher service level, which was the reason why the innovative Daily Maersk product was discontinued in 2015 (Porter, 2015).

The heuristic (Lee et al., 2015) used by the shipping lines for schedule design can be formulated as $x_i = D_i/v^p + \mu_i + K_i\sigma_i$, where D_i is the sailing distance of the ith leg; v^p is the planned maximum speed; μ_i and σ_i are the mean and standard deviation of stochastic port time; and K_i is a safety factor that denotes port contingency. K_i is set to distribute the total buffer time of a voyage to all ports. The total buffer time is the amount of time left after deducting the expected sailing times $\sum_{i=1}^{I} D_i/v^p$ and the expected port times $\sum_{i=1}^{I} \mu_i$ from the total voyage time. We set K_i equal at all ports to have a fair allocation of total buffer time. Given a total voyage time and the planned speed, it is easy to calculate K_i when the port time mean and variance are provided. For example, the voyage time for an 11-week service is 1,848 hours. Based on the data provided in Table 1, the expected total service times at all ports are 347.40 hours. The total sailing distance is 25,016 nautical miles. If the planned maximum speed is 20 knots, the total buffer time can be calculated as $1,848 - 25,016/20 - 347.4 = 249.80$ hours. Given that the standard deviations of port service times are summed up as 102.77 at all ports, K_i can be computed as $249.80/102.77 = 2.43$. Following the formula, schedule interval x_i for $i = 1, \ldots, 19$ can be calculated as 35.4 hours, 43.1 hours, ..., 159.2 hours, respectively.

Apparently, the higher the planned maximum speed is, the greater the total buffer time is with the same total voyage time, which leads to a more reliable schedule. Our COP model is flexible enough to set different headhaul and backhaul speeds. However, in this comparison, we follow the industry practice to set a same planned maximum speed at all legs (Lee et al., 2015; Song et al., 2015). In the COP model, the last port is assigned a weight, which is three times that of other ports to penalize a vessel returning late to the home port, therefore upholding the assumption that a vessel always starts a voyage on time.

Based on the same port time data provided in Table 1, we obtain COP schedules and heuristic schedules for multiple voyage times: 12 weeks, 11 weeks and 10 weeks. To ensure a fair comparison, we derive each pair of COP and heuristic schedules using the same planned maximum speed between 16 and 25 knots. Note that the planned maximum speed determines the upper bound of actual bunker consumption, which should not exceed the bunker budget. We run Simulation B, which allows dynamic speed adjustments at sea, to simulate the performance of some feasible schedules and summarize the results in Figure 6. Following the practice of Maersk Line, as mentioned earlier, we give an allowance of 12 hours to vessel arrivals when determining whether they are late. It is encouraging to see that, in almost all instances, the COP model outperforms the heuristic by at least five percentage points in schedule reliability under the same planned maximum speed. This suggests that the COP schedules can
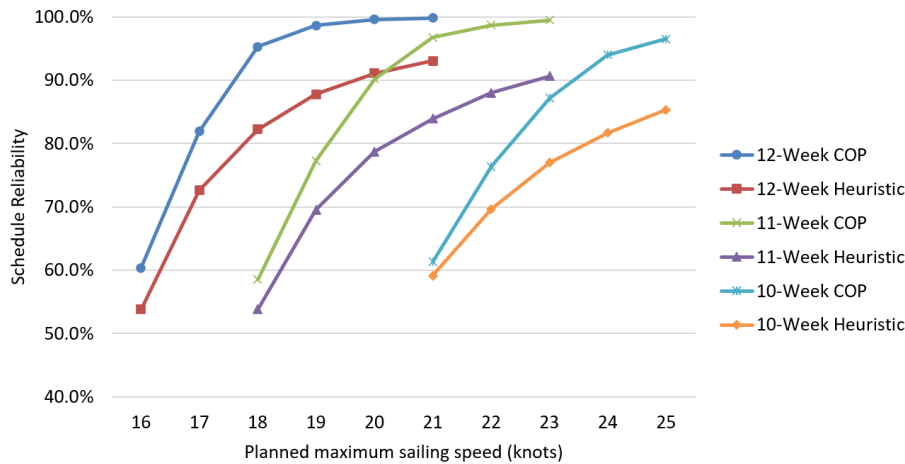
Figure 6: Trade-off between planned speed and schedule reliability

achieve higher schedule reliability given the same bunker budget.

Figure 6 shows the overall pattern in the relationships between the planned speed and schedule reliability. A higher planned speed helps improve schedule reliability. However, the marginal effect of a higher sailing speed on schedule reliability will decrease significantly as the on-time probability approaches about 80% using the heuristic for schedule design. This explains why the global schedule reliability in liner shipping is generally no better than 80% (Morley, 2019), avoiding burning a lot more bunker for slightly higher schedule reliability. It suggests that absolute reliability is a costly goal in practice. The same pattern is observed for schedules designed by the COP model. However, the COP model can achieve near-perfect schedule reliability when the planned speed is high enough for an 11-week or a 12-week service.

Figure 6 also reveals the impact of voyage time on schedule reliability. Schedule reliability improves substantially under the same planned speed when the voyage time is increased from 10 to 11 weeks or 11 to 12 weeks. This is because more buffer time is created in the schedule. For example, at the planned speed of 21 knots, the reliability of a COP schedule improves from 61.3% to 96.7% when the voyage time increases from 10 weeks to 11 weeks. The same pattern is observed using the heuristic for schedule design, albeit with poorer reliability than the COP model. Increasing the voyage time further to 12 weeks will push schedule reliability even higher to 99.6% for a COP schedule. However, the marginal benefit in schedule reliability is small because a voyage time of 11 weeks is already sufficient. This observation is in complete agreement with the theoretical analysis presented in Section 3.2.

Figure 7 illustrates the relationships between the planned speed and bunker consumption. The general pattern for both heuristic and COP schedules is that a higher sailing speed substantially increases bunker consumption. However, using heuristic schedules results in a much steeper increase in bunker consumption than using COP schedules. For example, when an 11-week service targets 80% schedule reliability, the required planned speed for the COP and heuristic schedules, which can be seen in Figure
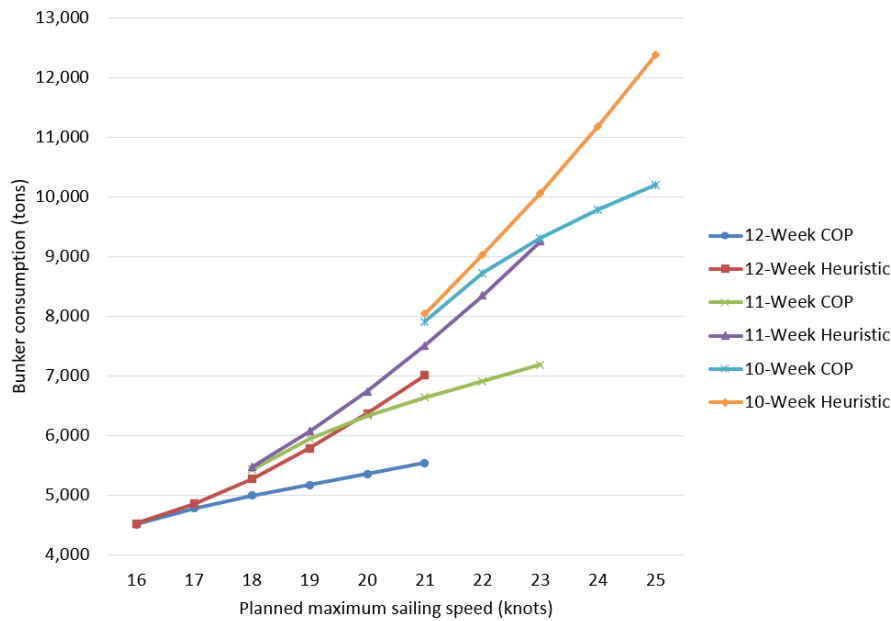
33

Figure 7: Trade-off between planned speed and bunker consumption

6, are about 19.3 and 20.3 knots, respectively. Their corresponding bunker consumptions, which can be seen in Figure 7, are about 6,100 and 6,900 tons. This means that the COP schedule can save the bunker by about 800 tons or 11.6% compared to the heuristic counterpart. The difference increases to about 2,700 tons (6,300 vs 9,000 tons) or 30% equivalent if targeting 90% schedule reliability. This shows that the COP model is most advantageous for designing schedules that require high schedule reliability. The reduced bunker consumption is beneficial not only for cost but also for environmental sustainability as it leads to lower emissions. Overall, the COP model performs much better than the heuristic schedule in balancing bunker consumption and sailing speed.

6   Managerial Insights

The theoretical analysis and numerical results presented above offer important managerial insights for the liner shipping schedule design. Firstly, there is great value in data and advanced modeling capabilities, as demonstrated in the outstanding performance of the distributionally robust COP model developed in this paper. Ocean carriers should collect port time and sailing time data because such data are very beneficial to schedule design. Planners can use historical data to aid the design of robust schedules. It is also worthwhile for ocean carriers to invest in advanced modeling capabilities to help with operations planning. Some of the leading ocean carriers, including Maersk Line, have developed advanced decision tools for schedule design. The innovative modeling approach presented in this study is especially advantageous for designing highly reliable service schedules. In the simulation experiments, our COP schedule outperforms the schedule reliability of a Daily Maersk service and, at the same time, reduces bunker consumption.

34

In comparison with a heuristic widely used for schedule design in liner shipping, our COP schedules can improve schedule reliability by at least 5% under the same bunker budget. If targeting at the same schedule reliability level, the COP schedules consume considerably less bunker, especially at a high service level requirement.

Secondly, despite its simplicity, the industry practice of using a constant nominal sailing speed (Lee et al., 2015) in timetable design coincides with the structural properties of a liner service schedule, which optimizes schedule reliability. This is a surprise but confirmed by Theorem 4. The same practice is still relevant when a shipping line differentiates headhaul and backhaul speeds. A shipping line can set the same speed for all the legs in the headhaul journey, and another speed for all the legs in the backhaul journey.

Thirdly, it is possible to improve schedule reliability by increasing the voyage time, but its marginal benefit will become small when the voyage time is no longer tight. This sheds light on the market and operations dynamics in the liner shipping industry in the early 2010s. During the time, slow steaming gained popularity due to an elevated bunker price (Maloni et al., 2013) and the mounting pressure to save bunker cost. When shipping lines reduced sailing speeds, they also increased the voyage time by deploying extra vessels in many service routes. Consequently, there was an improvement in schedule reliability in the liner shipping industry, although the overall service quality was still far from being ideal. Daily Maersk was the champion in improving schedule reliability, although it was short-lived. Our analysis results decode the operational strategies behind the Daily Maersk's promise of absolute reliability—it is indeed feasible to achieve near-perfect schedule reliability by adding extra vessels and slowing them down. When the voyage time is tight, the benefit of adding an extra vessel to schedule reliability can be significant. However, the marginal benefit will become small when the voyage time is no longer tight. Shipping lines need to find the right trade-off between vessel cost, bunker cost, and schedule reliability targets. Although the Daily Maersk product did succeed in fulfilling its absolute reliability promise, its operational cost was too high to be sustainable when the shippers were not willing to pay more for a higher service level.

Fourthly, there is a fundamental trade-off between the bunker budget and the reliability targets that can be achieved when the voyage time is fixed. With a generous bunker budget, a vessel can sail at high speed to reduce the sailing time, which in turn creates more buffer time for achieving better reliability performance. The innovative algorithm presented in Section 3.2 can help calibrate weights assigned to ports as inputs to the COP model for schedule design. When the bunker budget is generous, all reliability targets can be attained. However, an insufficient bunker budget cannot ensure the vessel to return to the home port with a reasonably high probability for starting the next voyage on time. Therefore, shipping lines need to set schedule reliability targets realistically in relation to their bunker budgets.

Last but not least, schedule reliability at hub ports can be protected by applying a simple but very

effective tactic derived from the numerical experiments, i.e., to allocate additional buffer time to the scheduled intervals, which are right before the hub ports. This tactic is useful for ensuring the overall reliability of the service networks because delays at hub ports affect many transshipment activities. The trade-off is a reduced probability of the vessel returning to the home port on time.

7   Conclusions

Liner shipping is the primary mode of transporting manufactured goods across continents. Its service quality has a direct impact on the global supply chain performance of many products. However, the liner shipping industry has long had a notorious reputation of schedule unreliability, mainly due to the ocean carriers' operational focus on cost as well as inherent uncertainties at sea and ports. The existing literature on liner shipping schedule design has focused on cost minimization, and limited attention has been given to incorporating schedule reliability in timetable design. In practice, shippers do care about schedule reliability, but few of them are willing to pay a premium price for a higher service level. Therefore, ocean carriers need to design reliable schedules without incurring a higher bunker consumption than their competitors or to design schedules that meet a schedule reliability target. To the best of our knowledge, this problem has not been adequately defined and investigated in the literature. This paper addresses this knowledge gap by formulating a distributionally robust model to optimize schedule reliability in liner shipping and using an innovative copositive program to solve the equivalent non-linear stochastic optimization problem.

While we focus on the static timetable design problem in the paper, we note that the model can be used in a real-time manner to guide the selection of sailing speed and schedule adjustment to downstream ports by re-solving the convex relaxation based on the latest update on the remaining voyage duration, latest estimates of the port and sailing delays, and also the remaining bunker budget available. In this way, the speed that we can use to solve the convex relaxation of the timetable design problem becomes an advantage. Nevertheless, this research also has its limitations. It focuses on a tactical level decision, timetable design, and does not consider recovery decisions at an operational level. To obtain the structural properties of the most reliable schedule, the analytical results require some assumptions to simplify the problem. Nevertheless, the model does capture the unique and complex delay propagation issue in liner shipping, and it can be easily extended to incorporate practical considerations, including transit time constraints and berthing time windows. The models developed in this study are for a single-liner shipping service. Future works need to extend the models for designing schedules of all services involved in a liner shipping network. The focus of this study is on schedule reliability. It is possible to relax some of the numerical experiments' assumptions to investigate further the trade-offs between bunker consumption, voyage time constraint, and schedule reliability in various practical settings. Depending

on the vessels being deployed, the bunker consumption function used in the model formulation may need to be calibrated or revised. We leave these and other issues to future research.

References

Agarwal, R., Ergun, O. (2008) *Ship scheduling and network design for cargo routing in liner shipping*, Transportation Science, Vol. 42, No. 2, pp. 175–196.

Agarwal, R., Ergun, O. (2010) *Network design and allocation mechanisms for carrier alliances in liner shipping*, Operations Research, Vol. 58, No. 6, pp. 1726–1742.

Ahipaşaoğlu, S. D., Arıkan, U., Natarajan, K. (2016) *On the flexibility of using marginal distribution choice models in traffic equilibrium*, Transportation Research Part B: Methodological, Vol. 91, pp. 130–158.

Aydin, N., Lee, H., Mansouri, S. A. (2017) *Speed optimization and bunkering in liner shipping in the presence of uncertain service times and time windows at ports*, European Journal of Operational Research, Vol. 259, No. 1, pp. 143–154.

Bertsimas, D., Sim, M., Zhang, M. (2019) *Outpatient-scheduling in health care: A review of literature*, Management Science, Vol. 65, No. 2, pp. 604–618.

Brouer, B. D., Karsten, C. V., Pisinger, D. (2015) Big data optimization in maritime logistics. In C.V. Karsten (Ed.), *Competitive Liner Shipping Network Design* (pp. 51-99). Kgs. Lyngby: DTU Management Engineering.

Cayirli, T., Veral, E. (2003) *Outpatient-scheduling in health care: A review of literature*, Production and Operations Management, Vol. 12, No. 4, pp. 519–549.

Christiansen, M., Fagerholt, K., Ronen, D. (2004) *Ship routing and scheduling: Status and perspectives*, Transportation Science, Vol. 38, No. 1, pp. 1–18.

Chen, Z., Kuhn, D., Wiesemann, W. (2020) *Data-driven chance constrained programs over Wasserstein balls*, Working Paper, Available from Optimization Online.

Delage, E., Ye., Y. (2019) *Distributionally robust optimization under moment uncertainty with application to data-driven problems*, Operations Research, Vol. 55, No. 3, pp. 596–612.

Drewry (2010) *Schedule reliability insight Q3*, Technical report, Drewry Shipping Consultants Ltd.

Drewry (2013) *Carrier performance insight,* Technical report, Drewry Shipping Consultants Ltd.

Du, Y., Chen, Q., Quan, X., Long, L., Fung, R. Y. K. (2011) *Berth allocation considering fuel consumption and vessel emissions*, Transportation Research Part E: Logistics and Transportation Review, Vol. 47, No. 6, pp. 1021–1037.

Du, Y., Meng, Q., Wang, Y. (2015). *Budgeting the fuel consumption of a container ship over a round voyage via robust optimization.* Transportation Research Record: Journal of the Transportation Research Board, Vol. 2477, pp. 68–75.

Fagerholt, K., Laporte, G., Norstad, I. (2010) *Reducing fuel emissions by optimizing speed on shipping routes*, Journal of the Operational Research Society, Vol. 61, No. 3, pp. 523–529.

Fransoo, J. C., Lee, C. -Y. (2013) *The Critical Role of Ocean Container Transportin Global Supply Chain Performance*, Production and Operations Management, Vol. 22, No. 2, pp. 253–268.

Gao, R., Kleywegt, A. J. (2016) *Distributionally robust stochastic optimization with Wasserstein distance*, arXiv preprint arXiv:1604.02199.

Gao, S. Y., Simchi-Levi, D., Yan, Z., Teo, C. -P. (2019) *Disruption risk mitigation in supply chain: The risk exposure index revisited*, Operations Research, Vol. 67, No. 3, pp. 831–852.

Gupta, D., Denton, B. (2008) *Appointment scheduling in health care: Challenges and opportunities*, IIE Transactions, Vol. 10, No. 9, pp. 800–819.

Hanasusanto, G., Kuhn, D. (2017) *Conic programming reformulations of two-stage distributionally robust linear programs over Wasserstein balls*, Operations Research, Vol. 66, No. 3, pp. 597–892.

Kjeldsen, K. (2011) Classification of ship routing and scheduling problems in liner shipping, INFOR, Vol. 49, No. 2, pp. 139–152.

Kong, Q., Lee, C. -Y., Teo, C. -P., Zheng, Z. (2013) *Scheduling arrivals to a stochastic service delivery system using copositive cones*, Operations Research, Vol. 61, No. 3, pp. 711–726.

Kuhn, D., Mohajerin Esfahani, P., Nguyen, V. A., Shafieezadeh-Abadeh, S. (2019) *Wasserstein distributionally robust optimization: Theory and applications in machine learning*, INFORMS 2019 TutORials in Operations Research.

Lam, J. S. L., van de Voorde, E. (2011) *Scenario analysis for supply chain integration in container shipping*, Maritime Policy and Management, Vol. 38, No. 7, pp. 705–725.

Leach, P. T. (2012) *Maersk plans other Daily Maersk services*, Available at http://www.joc.com/container-lines/maersk-plans-other-daily-maersk-services, Accessed on 28 May 2012.

Lee, C. -Y., Lee, H. L., Zhang, J. (2015) *The impact of slow ocean steaming on delivery reliability and fuel consumption*, Transportation Research Part E: Logistics and Transportation Review, Vol. 76, pp.176–190.

Li, X., Natarajan, K., Teo, C. -P., Zheng, Z. (2014) *Distributionally robust mixed integer linear programs: Persistency models with applications*, European Journal of Operational Research, Vol. 233, No. 3, pp. 459–473.

Li, C., Qi, X., Song, D. (2016) *Real-time schedule recovery in liner shipping service with regular uncertainties and disruption events*, Transportation Research Part B: Methodological, Vol. 93, pp. 762–788.

Lofberg, J. (2004) YALMIP: A toolbox for modeling and optimization in MATLAB, in Proceedings of the CACSD Conference, Taipei, Taiwan.

Maersk Line (2011) *Daily Maersk: Introducing absolute reliability*, Available at http://www.dailymaersk.com, Accessed on 15 February, 2012.

Maersk Line (2011) *Daily Maersk: Slow steaming - the full story*, Available at http://www.maersk.com/Innovation/WorkingWithInnovation/Documents/Slow%20Steaming%20-%20the%20full%20story.pdf, Accessed on 30 April, 2020.

Mak, H. Y., Rong, Y., Zhang, J. (2015) *Appointment scheduling with limited distributional information*, Management Science, Vol. 61, No. 2, pp. 316–334.

Maloni, M., Paul, J. A., Gligor, D. M. (2013) Slow steaming impacts on ocean carriers and shippers. Maritime Economics & Logistics, Vol. 15, No. 2, pp. 151–171.

Mishra, V. K., Natarajan, K., Padmanabhan, D., Teo, C. -P., Li, X. (2014) *On theoretical and empirical aspects of marginal distribution choice models*, Management Science, Special Issue on Business Analytics, Vol. 60, No. 6, pp. 1511–1531.

Mohajerin Esfahani, P., Kuhn, D. (2018) *Data-driven distributionally robust optimization using the Wasserstein metric: Performance guarantees and tractable reformulations*, Mathematical Programming, Vol. 117, pp. 115–166.

Morley, H. R. (2019) *Index to help shippers counter poor schedule reliability*, Available at https://www.joc.com/maritime-news/container-lines/index-help-shippers-counter-poor-schedule-reliability_20190905.html, Accessed on 30 March, 2020.

Mulder, J., Dekker, R. (2019) *Designing robust liner shipping schedules: Optimizing recovery actions and buffer times*, European Journal of Operational Research, Vol. 272, No. 1, pp. 132–146.

Mulder, J., van Jaarsveld, W., Dekker, R. (2019) *Simultaneous optimization of speed and buffer times with an application to liner shipping*, Transportation Science, Vol 53, No. 2, pp. 319–622.

Natarajan, K., Teo, C. -P., Zheng, Z. (2011) *Mixed 0-1 linear programs under objective uncertainty: A completely positive representation*, Operations Research, Vol. 59, No. 3, pp. 713–728.

Notteboom, T. (2006) *The time factor in liner shipping services*, Maritime Economics and Logistics, Vol. 8, No. 1, pp. 19–39.

Notteboom, T., Rodrigue, J. -P. (2008) *Containerisation, box logistics and global supply chains: The integration of ports and liner shipping networks*, Maritime Economics and Logistics, Vol. 10, No. 1/2, pp. 152–174.

Notteboom, T., Vernimmen, B. (2009) *The effect of high fuel costs on liner service configuration in container shipping*, Journal of Transport Geography, Vol. 17, No. 5, pp. 325–337.

Qi, X., Song, D. -P. (2012) *Minimizing fuel emissions by optimizing vessel schedules in liner shipping with uncertain port times*, Transportation Research Part E: Logistics and Transportation Review, Vol. 48, No. 4, pp. 863–880.

Qi, J. (2017) *Mitigating Delays and Unfairness in Appointment Systems*, Management Science, Vol. 63, No. 2, pp. 566–583.

Porter, J. (2015) *Premium 'Daily Maersk' service abandoned*, Available at https://www.lloydsloadinglist.com/freight-directory/news/Premium-Daily-Maersk-service-abandoned/61956.htm#.W0zXLtIzZPY, Accessed on 17 July, 2018.

Ronen, D. (2011) *The effect of oil price on containership speed and fleet size*, Journal of Operational Research Society, Vol. 62, No. 1, pp. 211–216.

Ronen, D. (1982) *The effect of oil price on the optimal speed of ships*, Journal of the Operational Research Society, Vol. 33, No. 11, pp. 1035–1040.

Song, D. -P., Li, D., Drake, P. (2015) *Multi-objective optimization for planning liner shipping service with uncertain port times*, Transportation Research Part E: Logistics and Transportation Review, Vol. 84, pp. 1–22.

Vernimmen, B., Dullaert, W., Engelen, S. (2007) *Schedule unreliability in liner shipping: Origins and consequences for the hinterland supply chain*, Maritime Economics and Logistics, Vol. 9, No. 3, pp. 193–213.

Wang, Y., Meng, Q., Kuang, H. (2013) *Jointly optimizing ship sailing speed and bunker purchase in liner shipping with distribution-free stochastic bunker prices*, Transportation Research Part C: Emerging Technologies, Vol. 89, pp. 35–52.

Wang, S., Meng, Q., Liu, Z. (2013) *Bunker consumption optimization methods in shipping: A critical review and extensions*, Transportation Research Part E: Logistics and Transportation Review, Vol. 53, pp. 49–62.

Wang, S., Meng, Q. (2012a) *Robust schedule design for liner shipping services*, Transportation Research Part E: Logistics and Transportation Review, Vol. 48, No. 6, pp. 1093–1106.

Wang, S., Meng, Q. (2012b) *Liner ship route schedule design with sea contingency time and port time uncertainty*, Transportation Research Part B: Methodological, Vol. 46, No. 5, pp. 615–633.

Wang, S., Meng, Q. (2012c) *Sailing speed optimization for container ships in a liner shipping network*, Transportation Research Part E: Logistics and Transportation Review, Vol. 48, No. 3, pp. 701–714.

Yan, Z., Gao, S. Y., Teo, C. -P. (2017) *On the design of sparse but efficient structures in operations*, Management Science, Vol. 64, No. 7, pp. 3421–3445.

Yao, Z., Ng, S. H., Lee, L. H. (2012) *A study on bunker fuel management for the shipping liner services*, Computers & Operations Research, Vol. 39, No. 5, pp. 1160–1172.

Zhang, A., Lam, J. S. L. (2015) *Daily Maersk'simpacts on shipper's supply chain inventories and implications for the liner shipping industry*, Maritime Policy & Management, Vol. 42, No. 3, pp. 246–262.

Zhang, A., Lam, J. S. L. (2014) *Impacts of Schedule Reliability and Sailing Frequency on the Liner Shipping and Port Industry*, Transportation Journal, Vol. 53, No. 2, pp. 235–253.

Appendix A. Technical Proofs

Proof of Proposition 1

From Theorem 3.3 in Natarajan et al. (2011), we can reformulate $\sup_{\phi \in \Omega(\tilde{\boldsymbol{\tau}}, \tilde{\boldsymbol{\epsilon}})} \mathbf{E}_\phi \left[f\left(\boldsymbol{x}, \boldsymbol{v}, \tilde{\boldsymbol{\tau}}, \tilde{\boldsymbol{\epsilon}} \right) \right]$ as a completely positive cone programming problem as follows:

$$
\begin{aligned}
&\sup_{\phi \in \Omega(\tilde{\boldsymbol{\tau}}, \tilde{\boldsymbol{\epsilon}})} \mathbf{E}_\phi \left[f\left(\boldsymbol{x}, \boldsymbol{v}, \tilde{\boldsymbol{\tau}}, \tilde{\boldsymbol{\epsilon}} \right) \right] \\
= \ &\sup \quad \boldsymbol{I}_I \bullet Y_u + \left(\boldsymbol{D} \circ \boldsymbol{u} - \boldsymbol{x} \right)^T \boldsymbol{y} \\
&s.t. \quad \begin{pmatrix} \boldsymbol{a}_i \\ -\boldsymbol{e}_i \end{pmatrix}^T \begin{pmatrix} \boldsymbol{y} \\ \boldsymbol{z} \end{pmatrix} = -w_{i+1}, \ \forall i = 1, 2, \ldots I \\
&\qquad \begin{pmatrix} \boldsymbol{a}_i \\ -\boldsymbol{e}_i \end{pmatrix}^T \begin{pmatrix} Y & Y_Z^T \\ Y_Z & Z \end{pmatrix} \begin{pmatrix} \boldsymbol{a}_i \\ -\boldsymbol{e}_i \end{pmatrix} = w_{i+1}^2, \ \forall i = 1, 2, \ldots I \\
&\qquad \begin{pmatrix} 1 & \boldsymbol{\mu}^T & \boldsymbol{y}^T & \boldsymbol{z}^T \\ \boldsymbol{\mu} & \Sigma & Y_u^T & Z_u^T \\ \boldsymbol{y} & Y_u & Y & Y_Z^T \\ \boldsymbol{z} & Z_u & Y_Z & Z \end{pmatrix} \succeq_{cp} 0
\end{aligned}
\tag{13}
$$

where the decision variables are $\boldsymbol{y} \in \mathbb{R}^I$, $\boldsymbol{z} \in \mathbb{R}^I$, and $Y, Y_u, Y_Z, Z, Z_u \in \mathbb{R}^{I \times I}$. The cone of completely matrix of dimension $n \times n$ is defined as $\left\{ A \in \mathbb{S}^{n \times n} : \exists \boldsymbol{v} \in \mathbb{R}_+^n, \text{ such that } A = \boldsymbol{v}\boldsymbol{v}^T \right\}$, where $\mathbb{S}^{n \times n}$ is the set of $n \times n$ symmetric matrices. We denote a completely positive matrix A as $A \succeq_{cp} 0$. The linear program over the cone of completely positive matrices is called completely positive program (CPP).

Taking the dual of the above CPP, we obtain the copositive program shown in the proposition. The strong duality follows from the generalized Slater's constraint qualification guaranteed by the technical assumption on $(1, \boldsymbol{\mu}, \Sigma)$ and the fact that $\sum_{i=1}^n \boldsymbol{a}_i \boldsymbol{a}_i^T$ is strictly copositive (Kong et al., 2013; Hanasusanto & Kuhn, 2017; Yan et al., 2017; Gao et al., 2019). The extension of the model to allow $(\tilde{\boldsymbol{\tau}} + \tilde{\boldsymbol{\epsilon}})$ to be negative follows from Theorem 4.1 established in Natarajan et al. (2011). As a result, the completely cone constraint in the above CPP is relaxed to

$$
\begin{pmatrix} 1 & \boldsymbol{\mu}^T & \boldsymbol{y}^T & \boldsymbol{z}^T \\ \boldsymbol{\mu} & \Sigma & Y_u^T & Z_u^T \\ \boldsymbol{y} & Y_u & Y & Y_Z^T \\ \boldsymbol{z} & Z_u & Y_Z & Z \end{pmatrix} \in \left\{ A \in \mathbb{S}^{(3I+1) \times (3I+1)} : \exists \boldsymbol{v} \in \mathbb{R}_+ \times \mathbb{R}^I \times \mathbb{R}_+^{2I}, \text{ such that } A = \boldsymbol{v}\boldsymbol{v}^T \right\},
$$

whose dual conic constraint is the one described in Remark 3 after Theorem 2.

Proof of Theorem 2

We only need to reformulate the bunker consumption budget constraint to complete the reformulation. Details of the transformation are shown below:

$$\sum_{i=1}^{I} D_i \left(k_1 v_i^2 + k_2 v_i + k_3 + \frac{k_4}{v_i} \right) \le B$$

$$\Longleftrightarrow \sum_{i=1}^{I} D_i \left(\frac{k_1}{u_i^2} + \frac{k_2}{u_i} + k_3 + k_4 u_i \right) \le B$$

$$\Longleftrightarrow \sum_{i=1}^{I} D_i \left[k_1 \left(\frac{1}{u_i} + \frac{k_2}{2k_1} \right)^2 - \frac{k_2^2}{4k_1} + k_3 + k_4 u_i \right] \le B$$

$$\Longleftrightarrow \exists g_i \ge 0, i = 1, 2 \ldots, I, \text{ such that } \begin{cases} \left(\frac{1}{u_i} + \frac{k_2}{2k_1} \right)^2 \le g_i, \forall i = 1, 2, \ldots, I \\ \sum_{i=1}^{I} D_i \left[k_1 g_i - \frac{k_2^2}{4k_1} + k_3 + k_4 u_i \right] \le B \end{cases}$$

The above two steps follow from $k_1 > 0$. To further reformulate the constraints, we introduce another auxiliary variable h_i:

$$\Longleftrightarrow \exists g_i, h_i \ge 0, i = 1, 2 \ldots, I, \text{ such that } \begin{cases} h_i^2 \le g_i, \forall i = 1, 2, \ldots, I \\ \frac{1}{u_i} + \frac{k_2}{2k_1} \le h_i, \forall i = 1, 2, \ldots, I \\ \sum_{i=1}^{I} D_i \left[k_1 g_i - \frac{k_2^2}{4k_1} + k_3 + k_4 u_i \right] \le B \end{cases}$$

For the above transformation to work, we need to show that at the optimal solution, $\frac{1}{u_i^*} + \frac{k_2}{2k_1} \ge 0$, where u_i^* denotes the optimal value of u_i. In general, we use the asterisk sign $(*)$ to indicate optimal solutions of corresponding decision variables. By our assumption that the bunker consumption eventually increases in sailing speed and there is room to save bunker by slowing down the vessel from the maximum speed, the maximum speed of a vessel is larger than the turning point even if the bunker consumption is decreasing in speed initially before the turning point. It can be easily verified that the turning point (if exists), will always be greater or equal to $-\frac{k_2}{2k_1}$, where the equality holds when $k_4 = 0$. Hence, we have $v_i^{max} \ge -\frac{k_2}{2k_1}$. If at the optimal solution, we have $\frac{1}{u_i^*} + \frac{k_2}{2k_1} < 0$ (in this case, $k_2 < 0$ since $k_1 > 0$), obviously h_i^* and g^* will be set to zero if the bunker consumption constraint is tight. Recall that $u_i^* = \frac{1}{v_i^*}$. Then one can always decrease u_i from u_i^* (equivalently, increase v_i from v_i^*) to the point that $\frac{1}{u_i} + \frac{k_2}{2k_1} = 0$ (equivalently, $v_i + \frac{k_2}{2k_1} = 0$) , since $v_i^{max} + \frac{k_2}{2k_1} \ge 0$. The values of h_i and g_i can still be kept at zero for the last constraint above to hold since $k_4 \ge 0$. By doing so, all the constraints will be honored including the original bunker consumption constraint. Since objective function of Problem (C), which equals to the objective function of its dual formulation in Eaquation (13) as a result of strong duality, is increasing in u_i (equivalently, decreasing in v_i), the objective value of Problem (C) can be reduced by decreasing

43

u_i from u_i^* to $-\frac{2k_1}{k_2}$. This contradicts the optimality of u_i^*. Therefore, at the optimal solution, we always have $\frac{1}{u_i^*} + \frac{k_2}{2k_1} \geq 0$. Such property allows us to reformulate the bunker consumption constraint as shown above and eventually convexify everything. We continue the transformation as follows:

$$\Longleftrightarrow \exists g_i, h_i \geq 0, i = 1, 2 \ldots, I, \text{ such that } \begin{cases} \begin{pmatrix} g_i & h_i \\ h_i & 1 \end{pmatrix} \succeq 0, \forall i = 1, 2, \ldots, I \\ \left(h_i - \frac{k_2}{2k_1} \right) u_i \geq 1, \forall i = 1, 2, \ldots, I \\ \sum\limits_{i=1}^{I} D_i \left[k_1 g_i - \frac{k_2^2}{4k_1} + k_3 + k_4 u_i \right] \leq B \end{cases}$$

$$\Longleftrightarrow \exists g_i, h_i \geq 0, i = 1, 2 \ldots, I, \text{ such that } \begin{cases} \begin{pmatrix} g_i & h_i \\ h_i & 1 \end{pmatrix} \succeq 0, \forall i = 1, 2, \ldots, I \\ \begin{pmatrix} h_i - \frac{k_2}{2k_1} & 1 \\ 1 & u_i \end{pmatrix} \succeq 0, \forall i = 1, 2, \ldots, I \\ \sum\limits_{i=1}^{I} D_i \left[k_1 g_i - \frac{k_2^2}{4k_1} + k_3 + k_4 u_i \right] \leq B \end{cases}$$

Combined the above constraints with the copositive constraint from Proposition 1, we have the results in Theorem 2.

Proof of Theorem 6

For the chosen $\boldsymbol{w}$, if $\lambda^*(\boldsymbol{w}) \leq 1 - \eta_{I+1}$, then by Corollary 5 and Algorithm SRA,

$$\hat{\eta}_i(\boldsymbol{w}) = 1 - \frac{\lambda^*(\boldsymbol{w})}{\lambda^*(\boldsymbol{w}) + w_i} = \frac{w_i}{1 - \bar{\eta}_{I+1} + w_i} = \eta_i, \forall i = 2, \ldots, I, \text{ and}$$

$$\hat{\eta}_{I+1}(\boldsymbol{w}) = 1 - \frac{\lambda^*(\boldsymbol{w})}{w_{I+1}} \geq \eta_{I+1}.$$

Thus, Problem (Q) is feasible.

On the other hand, suppose $\lambda^*(\boldsymbol{w}) > 1 - \eta_{I+1}$ but Problem (Q) is feasible. Then there exists $\tilde{\eta}_i \geq \eta_i$ for all i that can be obtained using a schedule, and the new targets are tight. Note that $\tilde{\eta}_i > \eta_i$ for at least some $i \in \{2, \ldots, I\}$, otherwise our earlier argument would have obtained the feasible schedule.

Let $\tilde{\boldsymbol{w}}$ be the corresponding weights obtained from Algorithm SRA for the new targets $\tilde{\eta}_i$, with converging fixed point $\lambda^*(\tilde{\boldsymbol{w}}) = 1 - \tilde{\eta}_{I+1}$ in the algorithm. Then $\lambda^*(\tilde{\boldsymbol{w}}) = 1 - \tilde{\eta}_{I+1} \leq 1 - \eta_{I+1} < \lambda^*(\boldsymbol{w})$. If we choose $\bar{\eta}_{I+1} = \tilde{\eta}_{I+1}$ in Algorithm SRA for the original target η_i, $i = 2, \ldots, I$, we would have calculated weight $w_i' = (1 - \tilde{\eta}_{I+1}) \frac{\eta_i}{1 - \eta_i} \leq (1 - \tilde{\eta}_{I+1}) \frac{\tilde{\eta}_i}{1 - \tilde{\eta}_i} = \tilde{w}_i$ for all $i = 2, \ldots, I$. Hence, $\hat{\eta}_{I+1}(\boldsymbol{w}') \geq \hat{\eta}_{I+1}(\tilde{\boldsymbol{w}})$, since the weights $w_{I+1}' = \tilde{w}_{I+1} = 1$ remain the same in both instances but $\tilde{\boldsymbol{w}}$ put higher weights on the reliability of all the ports except for the last port. Now $\lambda^*(\boldsymbol{w}') = 1 - \hat{\eta}_{I+1}(\boldsymbol{w}') \leq 1 - \hat{\eta}_{I+1}(\tilde{\boldsymbol{w}}) = \lambda^*(\tilde{\boldsymbol{w}}) = 1 - \tilde{\eta}_{I+1}$. From our argument on the existence of a unique fixed point in Algorithm SRA, the algorithm

44

would have converged to $1 - \bar{\eta}_{I+1} \leq 1 - \tilde{\eta}_{I+1} \leq 1 - \eta_{I+1}$, which contradicts the original assumption that the algorithm converges to $\lambda^*(\boldsymbol{w}) > 1 - \eta_{I+1}$.

Appendix B. Tables for Parameters and Results in Numerical Experiments

Port	Distance to Next Port (nm)	Port Time Mean (hour)	Port Time Variance (hour^2)	Sea Contingency Time (hour)	Sailing Delay Mean (hour)	Sailing Delay Variance (hour^2)
Busan	130	20.2	12.8	1.3	1.0	0.6
Hakata	626	8.0	2.4	6.3	5.0	14.2
Dalian	203	13.3	12.1	2.0	1.6	1.5
Xingang	471	19.1	46.4	4.7	3.8	8.1
Qingdao	454	15.4	66.9	4.5	3.6	7.5
Ningbo	134	12.5	24.0	1.3	1.1	0.7
Shanghai	835	14.5	40.0	8.4	6.7	25.3
Hong Kong	43	11.7	12.3	1.0	0.8	0.4
Yantian	1530	13.9	30.7	12.7	10.1	58.1
Tanjung Pelepas	5313	22.2	30.9	25.0	19.9	227.1
Suez Canal (Westbound)	3142	16.7	5.4	20.7	16.5	155.9
Le Havre	232	19.3	17.8	2.3	1.9	2.0
Rotterdam	212	20.2	19.7	2.1	1.7	1.6
Bremerhaven	85	24.3	35.8	1.0	0.8	0.4
Hamburg	372	25.8	109.3	3.7	3.0	5.0
Antwerp	137	25.5	71.2	1.4	1.1	0.7
Felixstowe	3258	23.6	65.5	21.3	17.0	164.7
Suez Canal (Eastbound)	5328	21.0	15.0	25.0	19.9	227.1
Singapore	2511	20.3	30.3	17.6	14.0	112.0

Source: Authors compiled based on data from Maersk Line, APL, OOCL, SeaRates.com and portworld.com.

Table 1: AE2 service data

Port	Weight I	Schedule I	On-time Prob		Weight II	Schedule II	On-time Prob		Weight III	Schedule III	On-time Prob	
			No DA	12hr DA			No DA	12hr DA			No DA	12hr DA
Busan	0.14	27.4	100.0%	100.0%	0.17	27.5	100.0%	100.0%	0.31	27.5	100.0%	100.0%
Hakata	0.14	45.2	48.3%	99.9%	0.17	45.2	48.7%	99.9%	0.31	45.2	49.1%	99.9%
Dalian	0.14	26.0	46.3%	99.2%	0.17	26.0	46.3%	99.2%	0.31	25.9	46.0%	99.2%
Xingang	0.14	47.9	40.7%	95.2%	0.17	47.9	40.3%	95.2%	0.31	47.8	39.8%	95.1%
Qingdao	0.14	45.5	45.7%	89.6%	0.17	45.1	45.6%	89.7%	0.31	44.8	45.2%	86.4%
Ningbo	0.14	22.6	50.0%	84.5%	0.17	22.7	48.9%	83.9%	0.31	22.1	47.7%	83.3%
Shanghai	0.14	67.4	44.2%	87.5%	0.17	67.9	43.7%	87.1%	0.31	68.4	38.1%	84.7%
Hong Kong	0.14	16.2	52.1%	86.6%	0.17	16.5	53.3%	87.1%	0.31	16.9	53.1%	86.5%
Yantian	0.14	103.1	40.0%	87.1%	0.17	107.3	41.6%	89.4%	0.31	118.5	46.2%	89.5%
Tanjung Pelepas	0.14	314.6	47.1%	79.2%	0.39	313.2	59.6%	88.6%	1.84	309.2	87.8%	97.2%
Suez Canal Westbound	0.14	204.1	52.9%	70.8%	0.17	207.8	54.0%	72.1%	0.31	213.3	51.4%	70.6%
Le Havre	0.14	37.1	63.5%	84.8%	0.17	42.2	76.5%	88.0%	0.31	54.5	83.0%	95.5%
Rotterdam	0.14	36.1	58.8%	88.8%	0.39	34.7	86.6%	95.5%	1.84	33.4	98.4%	99.7%
Bremerhaven	0.14	33.0	57.3%	91.3%	0.17	32.4	57.7%	95.6%	0.31	31.2	55.2%	99.4%
Hamburg	0.14	53.7	56.0%	92.7%	0.17	53.1	56.1%	95.5%	0.31	51.7	52.4%	97.4%
Antwerp	0.14	38.0	59.4%	89.1%	0.17	37.9	59.2%	89.0%	0.31	37.3	56.0%	84.9%
Felixstowe	0.14	210.7	54.8%	88.1%	0.17	211.0	53.8%	88.8%	0.31	210.7	51.1%	84.6%
Suez Canal Eastbound	0.14	328.4	56.6%	74.4%	0.17	325.6	57.5%	75.0%	0.31	319.5	56.0%	73.7%
Singapore	0.14	190.8	79.8%	91.9%	0.17	184.1	70.5%	87.9%	0.31	170.1	60.8%	82.7%
Busan	1		96.7%	99.3%	1		92.7%	98.2%	1		62.9%	85.2%
All Ports Average			57.5%	89.0%			59.6%	90.3%			59.0%	89.8%

Notes: Schedules in hours; Prob–probability; DA–delay allowance; I, II, and III refer to scenarios under Target Set I, Target Set II, and Target Set III, respectively.

Table 2: Hub port service reliability optimization (11-week voyage, design sailing speed 20 knots, simulation A)

Port	Uniform Distribution		Normal Distribution		Gamma Distribution		Two-point Distribution		Overall Average	
	Mean Delay	On-Time Prob	Mean Delay	On-Time Prob	Mean Delay	On-Time Prob	Mean Delay	On-Time Prob	Mean Delay	On-Time Prob
Busan	0.00	100.0%	0.00	100.0%	0.00	100.0%	0.00	100.0%	0.00	100.0%
Hakata	1.53	100.0%	1.47	99.3%	1.49	98.7%	2.03	100.0%	1.63	99.5%
Dalian	1.00	99.8%	1.01	99.4%	1.08	99.0%	1.81	100.0%	1.22	99.5%
Xingang	1.42	98.7%	1.44	98.1%	1.56	97.3%	2.36	100.0%	1.69	98.5%
Qingdao	2.32	97.2%	2.23	96.0%	2.50	94.2%	4.21	93.8%	2.82	95.3%
Ningbo	2.65	94.9%	2.58	94.1%	3.11	92.1%	4.87	87.3%	3.30	92.1%
Shanghai	3.00	91.1%	3.00	90.8%	3.67	88.6%	5.39	86.0%	3.77	89.1%
Hong Kong	1.79	96.1%	1.93	95.3%	2.72	93.0%	4.01	86.0%	2.61	92.6%
Yantian	2.28	95.9%	2.36	95.2%	3.16	93.0%	4.52	89.6%	3.08	93.4%
Tanjung Pelepas	0.79	98.7%	0.97	97.9%	1.57	96.2%	2.15	94.8%	1.37	96.9%
Suez Canal	0.12	99.8%	0.35	99.2%	0.58	98.4%	0.28	99.1%	0.33	99.1%
Le Havre	0.02	100.0%	0.06	99.9%	0.13	99.7%	0.00	100.0%	0.05	99.9%
Rotterdam	0.01	100.0%	0.04	99.9%	0.10	99.8%	0.00	100.0%	0.04	99.9%
Bremerhaven	0.74	100.0%	0.73	99.7%	0.86	99.1%	1.29	100.0%	0.91	99.7%
Hamburg	1.91	99.2%	1.70	97.6%	1.89	96.0%	2.77	100.0%	2.07	98.2%
Antwerp	2.55	94.9%	2.48	94.0%	2.93	92.4%	4.02	87.4%	3.00	92.2%
Felixstowe	3.61	87.5%	3.46	87.7%	4.08	85.6%	5.01	75.0%	4.04	84.0%
Suez Canal	1.06	97.2%	1.23	96.1%	1.61	94.9%	2.13	93.9%	1.50	95.5%
Singapore	0.01	100.0%	0.06	99.8%	0.10	99.7%	0.00	100.0%	0.04	99.9%
Busan	0.00	100.0%	0.01	100.0%	0.01	100.0%	0.00	100.0%	0.01	100.0%
All Ports Average	1.34	97.5%	1.36	97.0%	1.66	95.9%	2.34	94.6%	1.67	96.3%
Bunker Consumption (tons)	6,541		6,523		6,522		6,766		6,588	

Notes: Mean delay in hours; Prob–probability.

Table 3: Hub port service reliability optimization (Schedule II, Simulation B)

48

Port	Uniform Distribution		Normal Distribution		Gamma Distribution		Two-point Distribution		Overall Average
	Port Skipping Counts	On-Time Prob	Port Skipping Counts	On-Time Prob	Port Skipping Counts	On-Time Prob	Port Skipping Counts	On-Time Prob	On-Time Prob
Busan	0	100.0%	0	100.0%	0	100.0%	0	100.0%	100.0%
Hakata	0	100.0%	0	99.2%	0	98.8%	0	100.0%	99.5%
Dalian	0	99.9%	0	99.3%	0	99.2%	0	100.0%	99.6%
Xingang	0	98.6%	0	98.1%	0	97.6%	0	100.0%	98.6%
Qingdao	0	97.4%	0	96.3%	0	94.5%	0	92.8%	95.2%
Ningbo	0	94.7%	0	94.5%	0	92.4%	0	86.2%	92.0%
Shanghai	0	91.1%	0	91.9%	0	88.7%	0	85.9%	89.4%
Hong Kong	0	96.2%	0	95.9%	0	93.2%	0	86.8%	93.0%
Yantian	0	96.0%	0	95.5%	0	92.9%	0	89.7%	93.5%
Tanjung Pelepas	0	98.5%	0	98.1%	0	96.2%	0	94.9%	96.9%
Suez Canal	0	99.9%	0	99.0%	0	98.2%	0	99.2%	99.1%
Le Havre	0	100.0%	0	99.8%	0	99.6%	0	100.0%	99.9%
Rotterdam	0	100.0%	0	99.9%	0	99.7%	0	100.0%	99.9%
Bremerhaven	0	100.0%	0	99.6%	0	98.8%	0	100.0%	99.6%
Hamburg	1	99.2%	2	97.5%	5	95.7%	0	100.0%	98.1%
Antwerp	0	94.8%	0	94.4%	0	92.5%	0	87.3%	92.2%
Felixstowe	1	87.3%	0	86.8%	9	86.1%	0	75.5%	83.9%
Suez Canal	0	97.2%	0	96.3%	0	95.5%	0	94.3%	95.8%
Singapore	0	100.0%	0	99.8%	0	99.7%	0	100.0%	99.9%
Busan	0	100.0%	0	100.0%	0	100.0%	0	100.0%	100.0%
All Ports Average		97.5%		97.1%		96.0%		94.6%	96.3%
Bunker Consumption (tons)	6,530		6,508		6,528		6,770		6,584

Notes: Mean delay in hours; port skipping couts out of 5000 simulation runs; Prob–probability.

Table 4: Hub port service reliability optimization (Schedule II, Simulation C)

49

Port	Maersk Schedule (hr)	COP Weight	COP Schedule (hr)	COP Designed Speed (knots)	Schedule Difference (hr)
Busan	36.5	0.20	28.8	22.8	-7.7
Hakata	49.5	0.20	44.1	22.8	-5.4
Dalian	30.0	0.20	26.9	22.8	-3.1
Xingang	57.0	0.20	49.7	22.8	-7.3
Qingdao	71.0	0.20	54.2	22.8	-16.8
Ningbo	38.0	0.20	22.9	24.5	-15.1
Shanghai	70.0	0.20	65.7	24.5	-4.3
Hong Kong	26.0	0.20	18.2	24.5	-7.8
Yantian	90.0	0.20	94.6	24.5	4.6
Tanjung Pelepas	264.0	0.20	277.9	24.5	13.9
Suez Canal Westbound	173.0	0.20	186.2	24.5	13.2
Le Havre	41.0	0.20	36.6	24.5	-4.4
Rotterdam	67.0	0.20	54.3	22.8	-12.7
Bremerhaven	37.0	0.20	40.4	22.8	3.4
Hamburg	63.0	0.20	64.2	22.8	1.2
Antwerp	42.0	0.20	45.8	22.8	3.8
Felixstowe	195.0	0.20	208.2	22.8	13.2
Suez Canal Eastbound	313.0	0.20	324.1	22.8	11.1
Singapore	185.0	0.20	205.5	22.8	20.5
Busan		1			

Table 5: Comparison between the Maersk schedule and the COP schedule

50

Port	Uniform Distribution		Normal Distribution		Gamma Distribution		Two-point Distribution		Overall Average	
	Mean Delay	On-Time Prob	Mean Delay	On-Time Prob	Mean Delay	On-Time Prob	Mean Delay	On-Time Prob	Mean Delay	On-Time Prob
Busan	0.00	100.0%	0.00	100.0%	0.00	100.0%	0.00	100.0%	0.00	100.0%
Hakata	0.00	100.0%	0.00	100.0%	0.01	100.0%	0.00	100.0%	0.00	100.0%
Dalian	0.00	100.0%	0.00	100.0%	0.01	100.0%	0.00	100.0%	0.00	100.0%
Xingang	0.01	100.0%	0.04	100.0%	0.08	100.0%	0.00	100.0%	0.03	100.0%
Qingdao	0.00	100.0%	0.06	100.0%	0.15	99.8%	0.00	100.0%	0.05	99.9%
Ningbo	0.00	100.0%	0.00	100.0%	0.02	100.0%	0.00	100.0%	0.00	100.0%
Shanghai	0.00	100.0%	0.00	100.0%	0.01	100.0%	0.00	100.0%	0.00	100.0%
Hong Kong	0.03	100.0%	0.09	100.0%	0.17	99.8%	0.00	100.0%	0.07	99.9%
Yantian	0.00	100.0%	0.01	100.0%	0.03	100.0%	0.00	100.0%	0.01	100.0%
Tanjung Pelepas	1.92	96.5%	1.84	96.1%	1.92	95.5%	4.15	100.0%	2.46	97.0%
Suez Canal	3.70	86.7%	3.50	88.3%	3.61	87.8%	7.75	75.1%	4.64	84.5%
Le Havre	2.02	94.5%	2.12	93.4%	2.24	92.9%	4.23	87.5%	2.65	92.1%
Rotterdam	0.69	97.9%	0.95	97.0%	1.08	96.6%	2.12	93.7%	1.21	96.3%
Bremerhaven	0.00	100.0%	0.02	99.9%	0.03	99.9%	0.00	100.0%	0.01	100.0%
Hamburg	0.09	100.0%	0.28	99.8%	0.43	99.3%	0.00	100.0%	0.20	99.8%
Antwerp	0.01	100.0%	0.20	99.8%	0.48	98.9%	0.00	100.0%	0.17	99.7%
Felixstowe	0.40	100.0%	0.72	97.9%	1.18	95.8%	0.00	100.0%	0.58	98.4%
Suez Canal	0.28	99.9%	0.46	98.8%	0.65	98.2%	0.00	100.0%	0.35	99.2%
Singapore	0.00	100.0%	0.00	100.0%	0.00	100.0%	0.00	100.0%	0.00	100.0%
Busan	0.00	100.0%	0.00	100.0%	0.00	100.0%	0.00	100.0%	0.00	100.0%
All Ports Average	0.46	98.78%	0.51	98.55%	0.60	98.22%	0.91	97.81%	0.62	98.3%
Bunker Consumption (tons)	8,939		8,935		8,940		9,100		8,979	

Notes: Mean delay in hours; Prob–probability.

Table 6: Maersk AE2 schedule reliability performance

Port	Uniform Distribution		Normal Distribution		Gamma Distribution		Two-point Distribution		Overall Average	
	Mean Delay	On-Time Prob	Mean Delay	On-Time Prob	Mean Delay	On-Time Prob	Mean Delay	On-Time Prob	Mean Delay	On-Time Prob
Busan	0.00	100.0%	0.00	100.0%	0.00	100.0%	0.00	100.0%	0.00	100.0%
Hakata	0.61	100.0%	0.65	99.7%	0.72	99.4%	1.00	100.0%	0.75	99.8%
Dalian	0.18	100.0%	0.28	99.9%	0.35	99.8%	0.32	100.0%	0.28	99.9%
Xingang	0.31	100.0%	0.40	99.7%	0.52	99.3%	0.58	100.0%	0.45	99.7%
Qingdao	0.54	100.0%	0.63	99.5%	0.88	98.4%	1.13	100.0%	0.80	99.5%
Ningbo	0.03	100.0%	0.15	99.8%	0.46	98.9%	0.00	100.0%	0.16	99.7%
Shanghai	0.65	100.0%	0.83	98.7%	1.28	96.5%	0.87	100.0%	0.91	98.8%
Hong Kong	0.38	100.0%	0.49	99.4%	0.88	98.1%	0.54	100.0%	0.57	99.4%
Yantian	0.43	100.0%	0.58	99.5%	0.99	98.5%	0.51	100.0%	0.63	99.5%
Tanjung Pelepas	0.89	99.5%	0.95	98.4%	1.28	97.2%	2.11	100.0%	1.31	98.8%
Suez Canal	0.42	99.7%	0.63	98.3%	0.85	97.6%	0.39	100.0%	0.57	98.9%
Le Havre	0.01	100.0%	0.12	99.8%	0.22	99.5%	0.00	100.0%	0.09	99.8%
Rotterdam	0.11	100.0%	0.23	99.8%	0.39	99.4%	0.00	100.0%	0.18	99.8%
Bremerhaven	0.00	100.0%	0.00	100.0%	0.04	99.9%	0.00	100.0%	0.01	100.0%
Hamburg	0.00	100.0%	0.07	100.0%	0.18	99.8%	0.00	100.0%	0.06	99.9%
Antwerp	0.00	100.0%	0.13	99.9%	0.39	99.2%	0.00	100.0%	0.13	99.8%
Felixstowe	0.03	100.0%	0.27	99.3%	0.63	97.7%	0.00	100.0%	0.23	99.3%
Suez Canal	0.00	100.0%	0.04	100.0%	0.10	99.7%	0.00	100.0%	0.04	99.9%
Singapore	0.00	100.0%	0.00	100.0%	0.00	100.0%	0.00	100.0%	0.00	100.0%
Busan	0.00	100.0%	0.00	100.0%	0.00	100.0%	0.00	100.0%	0.00	100.0%
All Ports Average	0.23	100.0%	0.32	99.6%	0.51	99.0%	0.37	100.0%	0.36	99.6%
Bunker Consumption (tons)	7,867		7,841		7,854		8,247		7,952	

Notes: Mean delay in hours; Prob–probability.

Table 7: COP schedule reliability performance